



# Stationary Distribution, Extinction and Probability Density Function of a Stochastic Vegetation–Water Model in Arid Ecosystems

Baoquan Zhou<sup>1</sup> · Bingtao Han<sup>1</sup> · Daqing Jiang<sup>1,2</sup> · Tasawar Hayat<sup>2,3</sup> · Ahmed Alsaedi<sup>2,3</sup>

Received: 8 March 2021 / Accepted: 23 February 2022 / Published online: 26 March 2022

© The Author(s), under exclusive licence to Springer Science+Business Media, LLC, part of Springer Nature 2022

## Abstract

In this paper, we study a three-dimensional stochastic vegetation–water model in arid ecosystems, where the soil water and the surface water are considered. First, for the deterministic model, the possible equilibria and the related local asymptotic stability are studied. Then, for the stochastic model, by constructing some suitable stochastic Lyapunov functions, we establish sufficient conditions for the existence and uniqueness of an ergodic stationary distribution  $\varpi(\cdot)$ . In a biological interpretation, the existence of the distribution  $\varpi(\cdot)$  implies the long-term persistence of vegetation under certain conditions. Taking the stochasticity into account, a quasi-positive equilibrium  $\bar{D}^*$  related to the vegetation-positive equilibrium of the deterministic model is defined. By solving the relevant Fokker–Planck equation, we obtain the approximate expression of the distribution  $\varpi(\cdot)$  around the equilibrium  $\bar{D}^*$ . In addition, we obtain sufficient condition  $\mathcal{R}_0^E < 1$  for vegetation extinction. For practical application, we further estimate the probability of vegetation extinction at a given time. Finally, based on some actual vegetation data from Wuwei in China and Sahel, some numerical simulations are provided to verify our theoretical results and study the impact of stochastic noise on vegetation dynamics.

**Keywords** Stochastic vegetation–water model · Climatic variations · Stationary distribution · Ergodicity · Probability density function · Extinction

---

Communicated by Philipp M Altrock.

---

✉ Daqing Jiang  
daqingjiang2010@hotmail.com

<sup>1</sup> College of Science, China University of Petroleum (East China), Qingdao 266580, People's Republic of China

<sup>2</sup> Nonlinear Analysis and Applied Mathematics (NAAM)-Research Group, Department of Mathematics, King Abdulaziz University, Jeddah, Saudi Arabia

<sup>3</sup> Department of Mathematics, Quaid-i-Azam University 45320, Islamabad 44000, Pakistan

**Mathematics Subject Classification** 37M25 · 60H10 · 92B05 · 92D40

## 1 Introduction

Desertification, as a process of land degradation, is formed by human activity structure and irregular climatic variations under the condition of arid and semi-arid areas (London and Unep 1994). In recent few decades, land desertification has been one of the worldwide ecological environmental issues and become increasingly serious (Hautier et al. 2015). According to statistics reported by the United Nation's Division for Sustainable Development (UNSD), land desertification has led to a decline in living standards of approximately 25% of the world's population (Chen et al. 2021; Dai 2013). Worse yet, the area of semi-arid regions in recent years is at least 7% larger than that in 1960s (Huang et al. 2016). In particular, the total area of arid and semi-arid land accounts for about 24.6% of China (Li et al. 2004). Thus, an urgent task is to provide effective strategies to prevent land desertification and prompt the restoration of degraded ecosystems.

Theoretically, mathematical modeling is an important tool for studying the mechanism of desertification formation and providing some dynamical schemes to curb land desertification (Chen et al. 2021; Shnerb et al. 2003; May 1977; Marinov et al. 2013; Gilad et al. 2007; Saco et al. 2007; Kefi et al. 2008, 2010; Sun et al. 2013). Taking the evaporation of water and the consumption of herbivores into account, Shnerb et al. (2003) initially proposed a two-dimensional vegetation–water model, namely the S2003 model. Marinov et al. (2013) further studied the global stability of the possible equilibria of the S2003 model and obtained the existence of non-trivial periodic vegetation states when the rainfall rate maintains at an appropriate level. But in fact, most of the rain first falls on the soil surface and become soil water through the infiltration, then being absorbed by the plants through the capillary action of plant roots (Gilad et al. 2007). In this sense, Saco et al. (2007) introduced two monotonically increasing concave functions to describe the water infiltration and the capillary action of plant roots, respectively. Considering the additional root-augmentation feedback, Kefi et al. (2008, 2010) further established a three-variable vegetation–water model that distinguishes between soil water and surface water, which is usually named as K2008 model. Moreover, they analyzed the possible mechanism and bistability of desertification formation under three future climatic scenarios predicted by the Hadley Center Cox et al. (2000). Recently, Chen et al. (2021) applied the K2008 model to study the influences of temperature and precipitation change on the vegetation patterns of Wuwei (37.4N, 103.1E) in China. Moreover, it was numerically proved that the K2008 model can well describe the local vegetation state according to the local image of Wuwei taken from Google Earth.

However, the majority of the research results obtained by these models above are mainly experimental results, and there is a lack of quantitative analysis of the desertification restoration problem. That is to say, some theoretical dynamical behavior of a vegetation–water model should be analyzed for better practical application in arid and semi-arid ecosystems, such as long-term persistence of vegetation, vegetation extinction and the related mean extinction time. Thus, in this paper, we will show some

dynamical analysis for the existing vegetation–water models with good applicability (K2008 model as a case). Motivated by the idea of K2008 model mentioned in Chen et al. (2021), Kefi et al. (2008), Kefi et al. (2010), let  $P(t)$ ,  $W(t)$  and  $S(t)$  be the vegetation density ( $\text{g}/\text{m}^2$ ), soil water volume (mm) and surface water volume (mm) at time  $t$ , respectively. A deterministic vegetation–water model with non-runoff then takes the following form:

$$\begin{cases} \frac{dP(t)}{dt} = \frac{c\alpha_2 g_{\text{CO}_2} W(t)P(t)}{W(t) + k_1} - R_{\text{resp}} P(t), \\ \frac{dW(t)}{dt} = \frac{\alpha(P(t) + k_2 w_0)S(t)}{P(t) + k_2} - \frac{q\alpha_2 g_{\text{H}_2\text{O}} W(t)P(t)}{W(t) + k_1} - r_w W(t), \\ \frac{dS(t)}{dt} = R - \frac{\alpha(P(t) + k_2 w_0)S(t)}{P(t) + k_2}, \end{cases} \quad (1.1)$$

where  $R_{\text{resp}}$  is the average loss rate including consumption of herbivores and autotrophic respiration in plants.  $r_w$  denotes the average loss rate of soil water due to drainage and evaporation.  $R$  is the average rainfall rate. The infiltration capacity  $I_r$  of water is denoted by the term  $\frac{\alpha(P+k_2w_0)S}{P+k_2}$  with the maximum infiltration rate  $\alpha$  and the infiltration saturation constant  $k_2$ . Moreover,  $w_0 \in (0, 1)$  is the measure of the infiltration contrast between vegetated and bare soils. The term  $\frac{q\alpha_2 g_{\text{H}_2\text{O}} WP}{W+k_1}$  denotes the water conductance capacity  $T_r$ , which results from the difference between saturated and actual specific humidity.  $\alpha_2$  is the conversion rate of roots,  $q$  denotes the positive humidity difference, and  $k_1$  is the half-saturated constant of water uptake.  $g_{\text{CO}_2}$  and  $g_{\text{H}_2\text{O}}$  separately denotes the leaf conductance to  $\text{CO}_2$  and  $\text{H}_2\text{O}$ , which satisfy  $g_{\text{H}_2\text{O}} = \gamma g_{\text{CO}_2}$  with  $\gamma$  denoting the conversion coefficient for the molecular diffusivities of  $\text{CO}_2$  and  $\text{H}_2\text{O}$  Kefi et al. (2008). The term  $\frac{c\alpha_2 g_{\text{CO}_2} WP}{W+k_1}$  describes the carbon gain capacity of vegetation biomass, where  $c$  is the carbon gain rate. In addition, the units of the above parameters are presented in Table 1, and the relevant schematic diagram of system (1.1) is shown in Fig. 1.

In this paper, we define a critical value by  $\mathcal{R}_0 = \frac{c\alpha_2 g_{\text{CO}_2} R}{(R+r_w k_1) R_{\text{resp}}}$ . By a standard argument (Chen et al. 2021; Kefi et al. 2008), system (1.1) has a vegetation-free equilibrium  $D_0 = (P_0, W_0, S_0) = (0, \frac{R}{r_w}, \frac{R}{\alpha w_0})$ , which always exists. In addition to the equilibrium  $D_0$ , a unique vegetation-positive equilibrium  $D^* = (P^*, W^*, S^*) = (\frac{c}{q\gamma} (\frac{R}{R_{\text{resp}}} - \frac{r_w k_1}{c\alpha_2 g_{\text{CO}_2} - R_{\text{resp}}}), \frac{k_1 R_{\text{resp}}}{c\alpha_2 g_{\text{CO}_2} - R_{\text{resp}}}, \frac{R(P^* + k_2)}{\alpha(P^* + k_2 w_0)})$  will exist in system (1.1) when  $c\alpha_2 g_{\text{CO}_2} > R_{\text{resp}}$  and  $R > \frac{r_w k_1 R_{\text{resp}}}{c\alpha_2 g_{\text{CO}_2} - R_{\text{resp}}}$ , which are equivalent to  $\mathcal{R}_0 > 1$ .

It should be noted that the system (1.1) is established under a constant ecological environment. However, due to a continuous spectrum of disturbances in the actual situation (Beddington and May 1977), many of the main parameters in vegetation evolution, such as the rainfall rate, the intensity of grazing and the photosynthetic capacity, are not constants but rather fluctuate around some average values (Guttal and Jayaprakash 2007). Thus, it is important to study randomly perturbed vegetation–water models (Pan et al. 2022). So far, only a few stochastic vegetation–water models have been formulated to analyze the impact of stochastic noise on vegetation dynamics (Guttal and Jayaprakash 2008; Zhang et al. 2019; Han et al. 2014; Pan et al. 2020; Zhang et al. 2020). Specifically, Guttal and Jayaprakash (2008) established a two-

**Table 1** List of values of the physiological parameters of system (1.2) based on Wuwei (2001–2019) and Sahel (2002–2007)

Parameters	Description	Value	Unit	Source
$r_w$	The average loss rate of soil water	0.2	$m^2 \text{ day}^{-1}$	Chen et al. (2021), Kefi et al. (2008)
$\alpha$	The maximum infiltration rate	0.2	–	Chen et al. (2021), Kefi et al. (2008)
$k_2$	Infiltration saturation constant	5	$g \text{ m}^{-2}$	Chen et al. (2021), Kefi et al. (2008, 2010)
$w_0$	Infiltration ratio between vegetated and bare soil	0.2	$\text{day}^{-1}$	Chen et al. (2021), Kefi et al. (2008)
$\alpha_2$	Conversion rate of roots	$2.6 \times 10^{-2}$	$g^{-1} \text{ m}^2$	Chen et al. (2021), Kefi et al. (2008)
$g_{CO_2}$	Maximal leaf conductance to $CO_2$	$1 \times 10^{-2}$	$\text{mol m}^{-2} \text{ day}^{-1}$	Chen et al. (2021), Kefi et al. (2008)
$\gamma$	Conversion coefficient in diffusivities of $CO_2$ and $H_2O$	$2.59 \times 10^{-2}$	$\text{mm m}^{-2} \text{ mol}^{-1}$	Chen et al. (2021), Kefi et al. (2008)
$k_1$	Half-saturated constant of water uptake	5	$\text{mm day}^{-1}$	Chen et al. (2021), Kefi et al. (2008, 2010)
$\sigma_i \ (i = 1, 2, 3)$	The intensities stochastic noises	[0, 2]	–	Assumed

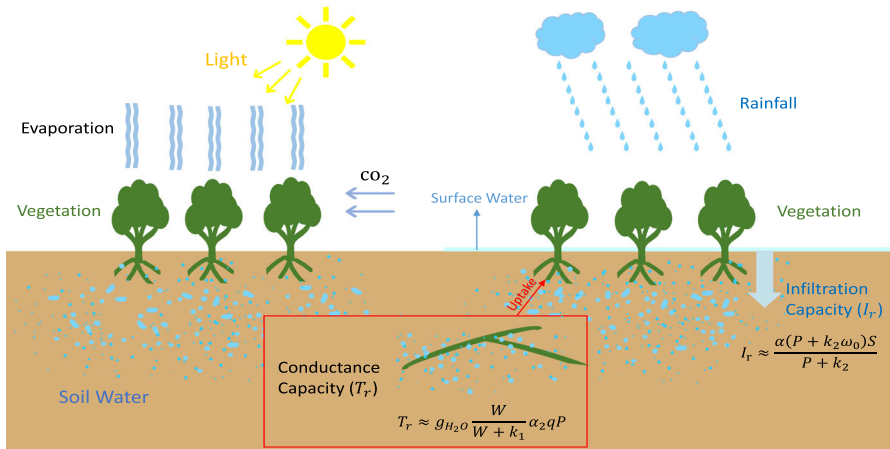


Fig. 1 The schematic diagram of deterministic vegetation–water system (1.1)

dimensional stochastic vegetation–water model with density-dependent effect, which is usually named as G2008 model. Recently, considering the random perturbations of the density-dependent effect and the rainfall rate, Zhang et al. (2019) developed a modified version of the G2008 model, and studied the transient dynamic properties of the stochastic system in terms of two important indexes including the first escape probability (FEP) and the mean first exit time (MFET). Moreover, it was numerically proved that the increase of noise intensity decreases basin stability of the vegetation–water system. Considering adding two factors, the pulse control strategy and the random perturbation of the growth response function of vegetation, in the G2008 model, Zhang et al. (2020) obtained the sufficient conditions for vegetation persistence and extinction in the mean sense. Based on the ecological model with runoff mentioned in Liu et al. (2019) and the linear perturbation approach proposed by Imhof and Walcher (2005), Pan et al. (2020) established a two-dimensional stochastic vegetation–water system with runoff, and theoretically obtained the sufficient and necessary conditions for the system’s near-optimal control problem (i.e., higher vegetation density and water density can be obtained at the lowest cost). Clearly, all the dimensions of the above stochastic vegetation–water models are no more than two dimensions.

As far as we know, no relevant investigations concerning the impact of stochastic noise on three-dimensional system (1.1) have been published yet, which is possibly resulted from the complexity of the system. Thus, in this paper, we will examine a stochastic version of system (1.1) from both transient and stationary dynamics perspectives. In practice, the loss rate  $R_{\text{esp}}$  of vegetation, the loss rate  $r_w$  of soil water and the rainfall rate  $R$  are three key parameters of vegetation evolution. In this sense,  $R_{\text{esp}}$ ,  $r_w$  and  $R$  should be regarded as three random variables  $\tilde{R}_{\text{esp}}$ ,  $\tilde{r}_w$  and  $\tilde{R}$ , respectively. Currently, the linear and second-order perturbation approaches are two well-established ways of introducing stochastic noise into biologically realistic dynamic models (Zhang and Zhang 2020; Liu et al. 2020; Cai et al. 2017; Zu et al. 2018; Han et al. 2020; Liu and Jiang 2018; Liu et al. 2018). Inspired by the fact, we assume that  $\tilde{R}_{\text{esp}}$ ,  $\tilde{r}_w$  and  $\tilde{R}$

separately fluctuate around the average values  $R_{\text{esp}}$ ,  $r_w$  and  $R$ , and satisfy

$$\begin{aligned} \text{(i)} \quad & -\tilde{R}_{\text{esp}}dt = -R_{\text{esp}}dt + \sigma_1dB_1(t), \\ \text{(ii)} \quad & -\tilde{r}_wdt = -r_wdt + \sigma_2dB_2(t), \quad \text{(iii).} \quad \tilde{R}dt = Rdt + \sigma_3S(t)dB_3(t), \end{aligned}$$

where  $B_i(t)$  ( $i = 1, 2, 3$ ) are three independent Brownian motions with  $\sigma_i > 0$  denoting their intensities. The expressions (i)–(ii) can be derived by the linear perturbation approach (Liu et al. 2020; Cai et al. 2017), and the form of (iii) is based on the second-order perturbation approach (Zu et al. 2018; Liu and Jiang 2018). From (i), for any time interval  $[t, t + \tau]$ ,  $-\tilde{R}_{\text{esp}}\tau$  is normally distributed with mean  $\mathbb{E}(-\tilde{R}_{\text{esp}}\tau) = -R_{\text{esp}}\tau$  and variance  $\text{Var}(-\tilde{R}_{\text{esp}}\tau) = \sigma_1^2\tau$ . Hence, the stochastic term  $-\tilde{R}_{\text{esp}}\tau$  will fluctuate around an average value  $-R_{\text{esp}}\tau$  for some small  $\tau$ , and its variance (i.e., the fluctuation intensity) will tend to zero if  $\tau \rightarrow 0$ , implying that (i) is a biologically reasonable assumption involved in the stochasticity. The analysis of (ii) can be completely analogous to (i). Moreover, the relevant biological explanation of (iii) can be obtained from Zu et al. (2018), Han et al. (2020) and is omitted here.

Thus, we replace  $-R_{\text{esp}}dt$ ,  $-r_wdt$  and  $Rdt$  in system (1.1) with  $-\tilde{R}_{\text{esp}}dt$ ,  $-\tilde{r}_wdt$  and  $\tilde{R}dt$ , respectively. Combined with (i)–(iii), the stochastic version of system (1.1) then takes the following form:

$$\begin{cases} dP(t) = \left[ \frac{c\alpha_2g_{\text{co}_2}W(t)P(t)}{W(t) + k_1} - R_{\text{esp}}P(t) \right]dt + \sigma_1P(t)dB_1(t), \\ dW(t) = \left[ \frac{\alpha(P(t) + k_2w_0)S(t)}{P(t) + k_2} - \frac{q\alpha_2\gamma g_{\text{co}_2}W(t)P(t)}{W(t) + k_1} - r_wW(t) \right]dt \\ \quad + \sigma_2W(t)dB_2(t), \\ dS(t) = \left[ R - \frac{\alpha(P(t) + k_2w_0)S(t)}{P(t) + k_2} \right]dt + \sigma_3S(t)dB_3(t), \end{cases} \quad (1.2)$$

where  $B_i(t)$  and  $\sigma_i$  ( $i = 1, 2, 3$ ) are the same as above. Moreover,  $B_i(t)$  ( $i = 1, 2, 3$ ) are all defined on a complete probability space  $\{\Omega, \mathcal{F}, \{\mathcal{F}_t\}_{t \geq 0}, \mathbb{P}\}$  with an increasing and right continuous  $\sigma$ -field filtration  $\{\mathcal{F}_t\}_{t \geq 0}$  (Mao 1997).

The primary purpose of this paper is to investigate system (1.2) from both long-term and transient dynamics perspectives. In the study of long-term dynamics of vegetation, on the one hand, the stability of the positive equilibrium state, which means that the vegetation in the deterministic model can stably coexist with other environmental variables (Marinov et al. 2013), is a very important topic in ecological protection. On the other hand, when stochastic noise is taken into account, the positive equilibrium states of most stochastic ecological models will no longer exist. Hence, there is a need to investigate the stability of the “stochastic positive equilibrium state” of stochastic vegetation–water models, namely the existence of a stationary distribution of their stochastic solutions (Pan et al. 2022). However, to the best of our knowledge, no relevant theoretical analysis has been reported yet in terms of the stability of the equilibria  $D_0$  and  $D^*$  in the deterministic system (1.1) and the existence of a stationary distribution of the stochastic system (1.2). To this end, in this paper, we will try to fill the gap. Furthermore, to better predict the statistical characteristics of vegetation dynamics

in arid ecosystems, such as the index FEP (Zhang et al. 2020a) of basin stability, the probability density function of the stationary distribution should be studied. In fact, the density function is determined by the Fokker–Planck equation, but the equation will often be difficult to solve for complex stochastic models. Thus, some new techniques should be developed to overcome the difficulty.

In the study of transient dynamics of vegetation, an interesting but challenging problem is to estimate the average residence time of the solution trajectory escaping from high vegetation state to low vegetation state even bare vegetation state (i.e., extinction) (Zhang et al. 2019), which can provide an early warning to make people take some effective measures such as artificial rainfall, to suppress the emergence of land desertification. So far, very few studies have directly analyzed the impact of stochastic noise on the average residence time of the state shifts of vegetation, and these analysis are only established under the stationary state shifts of several one-dimensional vegetation model (Zhang et al. 2020a, b). For example, Zhang et al. (2020a) first used a new signal, the maximum of the stationary probability density function (SPDF), to derive the analytical expression of the MFET escaping from high vegetation state to low vegetation state. In the present paper, we will generalize these results above to obtain the probability of vegetation extinction of system (1.2) at any given time, which is a new mathematical attempt in the study of transient dynamics of vegetation.

In comparison with the existing results, our main innovations and contributions are as follows. To better study the impact of stochastic noise on vegetation dynamics, we first use the Routh–Hurwitz criterion (Ma et al. 2015) to obtain the local stability of the equilibria  $D_0$  and  $D^*$  of system (1.1). Using Assumption (B) in Khasminskii (2011) and the strong law of large numbers (Lipster 1980), we construct some appropriate stochastic Lyapunov functions to obtain a critical value  $\mathcal{R}_0^H$  and prove that system (1.2) has a unique ergodic stationary distribution if  $\mathcal{R}_0^H > 1$ . Using novel techniques (i.e., combining Lemma 2.6 in Zhou et al. (2021) and the transformation theory of matrix algebra), we further derive an approximate expression of a local density function of the stationary distribution and combine a number of numerical examples to illustrate that the approximate local density function has a good global fitting effect for the realistic probability density function under some small stochastic noises. Another critical value  $\mathcal{R}_0^E$  is defined, and it is theoretically proved that the vegetation will be exponentially extinct for any positive initial conditions when  $\mathcal{R}_0^E < 1$ . Furthermore, the exact expression of the probability of vegetation extinction of system (1.2) at any given time is derived based on the stochastic comparison theorem (Ikeda and Watanabe 1977). Under the precise condition that required in practical need, we estimate the maximal extinction time of vegetation.

The rest of our paper is organized as follows. We introduce some necessary mathematical notations and lemmas in Sect. 2. In Sect. 3, the existence and uniqueness of an ergodic stationary distribution  $\varpi(\cdot)$  of the solution of system (1.2) is studied. By defining a quasi-positive equilibrium  $\overline{D}^*$  related to  $D^*$ , Sect. 4 shows that the stationary distribution around the equilibrium  $\overline{D}^*$  can be approximated by a log-normal distribution. Moreover, the explicit form of its log-normal density function is obtained. In Sect. 5, we establish sufficient criterion  $\mathcal{R}_0^E < 1$  for vegetation extinction, and the probability of extinction at a given time is calculated. Using some actual data from

Sahel, Yushu and Wuwei, Sect. 6 shows some numerical simulations to verify our theoretical results, and the impact of stochastic noise on the vegetation stability is investigated. Conclusion and further discussion are shown in Sect. 7. The local stability of deterministic system (1.1) is discussed in ‘‘Appendix A.’’

## 2 Preliminary

Throughout this paper, unless otherwise specified, let  $\mathbb{R}^l$  and  $\|\cdot\|$  be the  $l$ -dimensional Euclidean space and the Euclidean norm, respectively. We define  $\mathbb{R}_+^l = \{(x_1, \dots, x_l) \in \mathbb{R}^l | x_j > 0, 1 \leq j \leq l\}$ . If  $A$  is vector or matrix, its transpose is denoted by  $A^T$ . If  $A$  is a square matrix, let  $A^{-1}$  and  $\phi_A(\cdot)$  be its inverse matrix and characteristic polynomial, respectively. If  $A$  is a real symmetric matrix, we define

- $A \succ \mathbf{0}$  :  $A$  is a positive definite matrix,
- $A \succeq \mathbf{0}$  :  $A$  is at least a positive semi-definite matrix.

For any  $(a_1, a_2, \dots, a_l) \in \mathbb{R}^l$ , let  $a_1 \vee a_2 \vee \dots \vee a_n := \max_{1 \leq i \leq n} \{a_i\}$  and  $a_1 \wedge a_2 \wedge \dots \wedge a_n := \min_{1 \leq i \leq n} \{a_i\}$ . The one-dimensional standard normal distribution function is denoted by  $\Phi(\cdot)$ , namely  $\Phi(x) = \frac{1}{\sqrt{2\pi}} \int_{-\infty}^x e^{-\frac{t^2}{2}} dt$ , where  $x \in \mathbb{R}$ . Let  $\Phi^{-1}(\chi) := \Phi_\chi$  be the  $\chi$ -quantile of  $\Phi(\cdot)$ , such as  $\Phi_{0.975} = 1.96$  and  $\Phi_{0.01} = -2.326$ .  $\mathbb{P}\{\cdot\}$  denotes the probability measure of the complete probability space  $\{\Omega, \mathcal{F}, \{\mathcal{F}_t\}_{t \geq 0}, \mathbb{P}\}$ . Moreover, we define  $Q(t) = (P(t), W(t), S(t))^T$  as the solution of system (1.2) with the initial value  $(P(0), W(0), S(0))^T = Q(0)$ .

By a standard argument (Zhou et al. 2021) and the Routh–Hurwitz criterion (Ma et al. 2015), we obtain the following:

**Definition 2.1** (Ma et al. 2015)  $A$  is called a three-dimensional Hurwitz matrix if and only if  $A$  has all negative real part eigenvalues, that is,  $a_1 > 0, a_3 > 0$  and  $a_1 a_2 - a_3 > 0$ , where  $a_i$  ( $i = 1, 2, 3$ ) are the coefficients of  $\phi_A(\lambda) = \lambda^3 + a_1 \lambda^2 + \dots + a_2 \lambda + a_3$ . In this case, we write  $A \in \overline{RH}(3)$ .

**Lemma 2.1** (Zhou et al. 2021) For any three-dimensional real matrices  $A = (a_{ij})_{3 \times 3}$ ,  $\Lambda_0 = \text{diag}\{\delta_1^2, \delta_2^2, \delta_3^2\}$ , where  $\delta_k \neq 0$  ( $k = 1, 2, 3$ ). If  $\Sigma_0$  is a symmetric matrix, for the three-dimensional algebraic equation

$$\Lambda_0 + A \Sigma_0 + \Sigma_0 A^T = 0. \tag{2.1}$$

If  $A \in \overline{RH}(3)$ , then  $\Sigma_0$  is unique and  $\Sigma_0 \succ \mathbf{0}$ .

Let  $Z(t)$  be a homogeneous Markov process satisfying the following stochastic differential equation (SDE):

$$dZ(t) = b(Z(t))dt + f(Z(t))d\overline{B}(t), \tag{2.2}$$



where the drift term  $b(Z) : \mathbb{R}^l \rightarrow \mathbb{R}^l$  and the diffusion term  $f(Z) = (f_j^{(i)}(Z))_{l \times l} : \mathbb{R}^l \rightarrow \mathbb{R}^{l \times l}$  are both Borel measurable.  $f_j^{(i)}(Z)$  denotes the  $i$ th element of the  $j$ th column of the diffusion term  $f(\cdot)$ .  $\bar{B}(t)$  denotes a  $l$ -dimensional Brownian motion defined on the probability space  $\{\Omega, \mathcal{F}, \{\mathcal{F}_t\}_{t \geq 0}, \mathbb{P}\}$ . By a standard argument (Khasminskii 2011; Gard 1988), system (2.2) has a diffusion matrix  $F_0(Z) = f(Z)f^T(Z) := (\psi_{ij})_{l \times l}$ , where  $\psi_{ij} = \sum_{k=1}^n f_k^{(i)}(Z)f_k^{(j)}(Z)$ .

**Lemma 2.2** (Khasminskii 2011; Zhu and Yin 2007; Gard 1988) *If there exists a bounded domain  $\mathbb{G}_0 \subset \mathbb{R}^l$  with a regular boundary  $\Gamma_0$  satisfying the following conditions:*

( $\mathcal{A}_1$ ). *There is a non-negative  $C^2$ -Lyapunov function  $V(z)$  such that  $\mathcal{L}V(z)$  is negative for any  $z \in \mathbb{R}^l \setminus \mathbb{G}_0$ ,*

( $\mathcal{A}_2$ ). *There is a positive number  $m_0$  such that  $\sum_{i,j=1}^l \psi_{ij}(z)\zeta_i\zeta_j \geq m_0\|\zeta\|^2, \forall z \in \mathbb{G}_0; \zeta = (\zeta_1, \dots, \zeta_l) \in \mathbb{R}^l$ ,*

*then the Markov process  $Z(t)$  of system (2.2) is ergodic and has a unique stationary distribution  $\vartheta(\cdot)$  on  $\mathbb{R}^l$ , or rather  $Z(t)$  has a unique ergodic stationary distribution  $\vartheta(\cdot)$  on  $\mathbb{R}^l$ . In addition, by the ergodicity theorem Nguyen et al. (2020) and the strong law of large numbers, one has*

$$\mathbb{P} \left\{ \lim_{t \rightarrow \infty} \frac{1}{t} \int_0^t r(Z(t))dt = \int_{\mathbb{R}^l} r(z)\vartheta(dz) \right\} = 1,$$

where  $r(\cdot)$  be an integrable function with respect to the distribution  $\vartheta(\cdot)$ .

In practical terms,  $P, W$  and  $S$  represent the numbers of different kinds of subpopulations, which means that the solution  $Q(t)$  of system (1.2) should be global and non-negative. Hence, we must first give the existence and uniqueness of global solution to systems (1.2). Since the proof is similar to that of Theorem 2.1 in Gao et al. (2021), we omit it here and only state the related result.

**Lemma 2.3** *For any initial value  $Q(0) \in \mathbb{R}_+^3$ , system (1.2) has a unique solution  $Q(t)$  on  $t \geq 0$  and the solution will remain in  $\mathbb{R}_+^3$  with probability 1, namely  $(P(t), W(t), S(t)) \in \mathbb{R}_+^3$  for any  $t \geq 0$  almost surely (a.s.).*

From now on, unless specifically stated, we always assume that  $Q(0) \in \mathbb{R}_+^3$  for system (1.2).

### 3 Existence of Ergodic Stationary Distribution

In this section, we will investigate the stability of stochastic positive equilibrium state of system (1.2), i.e., the existence of an ergodic stationary distribution of system (1.2). First, we define

$$\mathcal{R}_0^H = \frac{c\alpha_2 g_{\text{CO}_2} r_w \alpha w_0 R}{(R + r_w k_1) \left( r_w + \frac{\sigma_2^2}{2} \right) \left( \alpha w_0 + \frac{\sigma_3^2}{2} \right) \left( R_{\text{esp}} + \frac{\sigma_1^2}{2} \right)}.$$

**Theorem 3.1** *If  $\mathcal{R}_0^H > 1$ , then the solution  $Q(t)$  of system (1.2) has a unique ergodic stationary distribution  $\varpi(\cdot)$  on  $\mathbb{R}_+^3$ .*

**Proof** By Lemma 2.3, we determine that system (1.2) has a unique global positive solution  $Q(t) \in \mathbb{R}_+^3$ . Hence, all of the descriptions of the space  $\mathbb{R}^l$  of Lemma 2.2 should be modified as  $\mathbb{R}_+^3$  in the following proof. We divide the proof of Theorem 3.1 into three steps. The first step is to construct a suitable  $C^2$ -Lyapunov function  $V(P, W, S)$ . The second is to use the function  $V(P, W, S)$  to verify condition  $(\mathcal{A}_1)$  in Lemma 2.2, and the third is to prove condition  $(\mathcal{A}_2)$  in Lemma 2.2.

**Step 1.** We define a  $C^2$ -Lyapunov function  $\bar{V}(P, W, S) : \mathbb{R}_+^3 \rightarrow \mathbb{R}$  by

$$\begin{aligned} \bar{V}(P, W, S) &= M_0 \left[ -\ln P + b_1(W + S) - b_2 \ln W - b_3 \ln S \right] \\ &\quad + \frac{1}{\theta + 1} \left( P + \frac{cW}{q\gamma} + \frac{2cS}{q\gamma} \right)^{\theta + 1} - \ln W - \ln S \\ &:= M_0 V_1(P, W, S) + V_2(P, W, S) + V_3(W, S), \end{aligned}$$

where  $V_1(P, W, S) = -\ln P + b_1(W + S) - b_2 \ln W - b_3 \ln S$ ,  $V_2(P, W, S) = \frac{1}{\theta + 1} \left( P + \frac{cW}{q\gamma} + \frac{2cS}{q\gamma} \right)^{\theta + 1}$  and  $V_3(W, S) = -\ln W - \ln S$ . The positive constants  $b_i$  ( $i = 1, 2, 3$ ) are determined in (3.5), and  $M_0 > 0$  is a sufficiently large constant satisfying the inequality (3.8). In addition,  $\theta > 0$  satisfies the following condition:

$$\beta_0 := \left( R_{\text{resp}} \wedge r_w \wedge \frac{\alpha w_0}{2} \right) - \frac{\theta}{2} (\sigma_1^2 \vee \sigma_2^2 \vee \sigma_3^2) > 0. \tag{3.1}$$

Note that the function  $\bar{V}(P, W, S)$  tends to  $\infty$  as  $(P, W, S)$  approaches the boundary of  $\mathbb{R}_+^3$  or as  $\|(P, W, S)\| \rightarrow \infty$ . Thus, there exists a point  $(P^0, W^0, S^0)$  in the interior of  $\mathbb{R}_+^3$ , at which  $\bar{V}(P, W, S)$  will be minimized. A non-negative  $C^2$ -Lyapunov function  $V(P, W, S)$  can then be constructed as follows:

$$V(P, W, S) = \bar{V}(P, W, S) - \bar{V}(P^0, W^0, S^0).$$

Applying the Itô’s formula (cf. Mao 1997) to  $-\ln W$ ,  $-\ln S$  and  $W + S$ , we calculate that

$$\begin{aligned} \mathcal{L}(-\ln W) &= -\frac{\alpha(P + k_2 w_0)S}{(P + k_2)W} + \frac{q\alpha_2 \gamma g_{\text{CO}_2} P}{W + k_1} + r_w + \frac{\sigma_2^2}{2} \\ &\leq -\frac{\alpha k_2 w_0 S}{(P + k_2)W} + \frac{q\alpha_2 \gamma g_{\text{CO}_2} P}{k_1} + r_w + \frac{\sigma_2^2}{2}. \end{aligned} \tag{3.2}$$

$$\mathcal{L}(-\ln S) = -\frac{R}{S} + \frac{\alpha(P + k_2 w_0)}{P + k_2} + \frac{\sigma_3^2}{2} \leq -\frac{R}{S} + \left( \alpha w_0 + \frac{\sigma_3^2}{2} \right) + \frac{\alpha P}{k_2}. \tag{3.3}$$

$$\mathcal{L}(W + S) = R - \frac{q\alpha_2 \gamma g_{\text{CO}_2} W P}{W + k_1} - r_w W \leq (R + r_w k_1) - r_w(W + k_1). \tag{3.4}$$

Combining (3.2)–(3.4), we have

$$\begin{aligned}
 \mathcal{L}V_1 &\leq \left(-\frac{c\alpha_2 g_{\text{CO}_2} W}{W + k_1} + R_{\text{esp}} + \frac{\sigma_1^2}{2}\right) \\
 &\quad + b_1[(R + r_w k_1) - r_w(W + k_1)] + b_2\left[-\frac{\alpha k_2 w_0 S}{(P + k_2)W} + \frac{q\alpha_2 \gamma g_{\text{CO}_2} P}{k_1}\right. \\
 &\quad \left.+ r_w + \frac{\sigma_2^2}{2}\right] + b_3\left[-\frac{R}{S} + \left(\alpha w_0 + \frac{\sigma_3^2}{2}\right) + \frac{\alpha}{k_2} P\right] \\
 &\quad - b_4(P + k_2) + b_4(P + k_2) \\
 &= -\left[\frac{c\alpha_2 g_{\text{CO}_2} W}{W + k_1} + b_1 r_w(W + k_1) + \frac{b_2 \alpha k_2 w_0 S}{(P + k_2)W} + \frac{b_3 R}{S} + b_4(P + k_2)\right] \\
 &\quad + \left(R_{\text{esp}} + \frac{\sigma_1^2}{2}\right) + b_1(R + r_w k_1) \\
 &\quad + b_2\left(r_w + \frac{\sigma_2^2}{2}\right) + b_3\left(\alpha w_0 + \frac{\sigma_3^2}{2}\right) + b_4 k_2 \\
 &\quad + \left(b_4 + \frac{b_3 \alpha}{k_2} + \frac{b_2 q \alpha_2 \gamma g_{\text{CO}_2}}{k_1}\right) P \\
 &\leq -5\sqrt[5]{\frac{c\alpha_2 g_{\text{CO}_2} W}{W + k_1} \cdot b_1 r_w(W + k_1) \cdot \frac{b_2 \alpha k_2 w_0 S}{(P + k_2)W} \cdot \frac{b_3 R}{S} \cdot b_4(P + k_2)} \\
 &\quad + \left(R_{\text{esp}} + \frac{\sigma_1^2}{2}\right) + b_1(R + r_w k_1) \\
 &\quad + b_2\left(r_w + \frac{\sigma_2^2}{2}\right) + b_3\left(\alpha w_0 + \frac{\sigma_3^2}{2}\right) + b_4 k_2 \\
 &\quad + \left(b_4 + \frac{b_3 \alpha}{k_2} + \frac{b_2 q \alpha_2 \gamma g_{\text{CO}_2}}{k_1}\right) P \\
 &= -5\sqrt[5]{c\alpha_2 g_{\text{CO}_2} r_w \alpha k_2 w_0 R b_1 b_2 b_3 b_4} \\
 &\quad + \left(R_{\text{esp}} + \frac{\sigma_1^2}{2}\right) + b_1(R + r_w k_1) \\
 &\quad + b_2\left(r_w + \frac{\sigma_2^2}{2}\right) + b_3\left(\alpha w_0 + \frac{\sigma_3^2}{2}\right) + b_4 k_2 \\
 &\quad + \left(b_4 + \frac{b_3 \alpha}{k_2} + \frac{b_2 q \alpha_2 \gamma g_{\text{CO}_2}}{k_1}\right) P.
 \end{aligned}$$

Let

$$\begin{aligned}
 b_1(R + r_w k_1) &= b_2\left(r_w + \frac{\sigma_2^2}{2}\right) = b_3\left(\alpha w_0 + \frac{\sigma_3^2}{2}\right) = b_4 k_2 \\
 &= \frac{c\alpha_2 g_{\text{CO}_2} r_w \alpha w_0 R}{(R + r_w k_1)\left(r_w + \frac{\sigma_2^2}{2}\right)\left(\alpha w_0 + \frac{\sigma_3^2}{2}\right)}.
 \end{aligned}$$

The solution of the above equations is unique, and it is

$$\begin{aligned}
 b_1 &= \frac{c\alpha_2 g_{co_2} r_w \alpha w_0 R}{(R + r_w k_1)^2 (r_w + \frac{\sigma_2^2}{2})(\alpha w_0 + \frac{\sigma_3^2}{2})}, & b_2 &= \frac{c\alpha_2 g_{co_2} r_w \alpha w_0 R}{(R + r_w k_1)(r_w + \frac{\sigma_2^2}{2})^2 (\alpha w_0 + \frac{\sigma_3^2}{2})}, \\
 b_3 &= \frac{c\alpha_2 g_{co_2} r_w \alpha w_0 R}{(R + r_w k_1)(r_w + \frac{\sigma_2^2}{2})(\alpha w_0 + \frac{\sigma_3^2}{2})^2}, & b_4 &= \frac{c\alpha_2 g_{co_2} r_w \alpha w_0 R}{(R + r_w k_1)(r_w + \frac{\sigma_2^2}{2})(\alpha w_0 + \frac{\sigma_3^2}{2})k_2}.
 \end{aligned}
 \tag{3.5}$$

Then, we obtain

$$\begin{aligned}
 \mathcal{L}V_1 &\leq - \frac{c\alpha_2 g_{co_2} r_w \alpha w_0 R}{(R + r_w k_1)(r_w + \frac{\sigma_2^2}{2})(\alpha w_0 + \frac{\sigma_3^2}{2})} + \left( R_{\text{esp}} + \frac{\sigma_1^2}{2} \right) \\
 &\quad + \left( b_4 + \frac{b_3 \alpha}{k_2} + \frac{b_2 q \alpha_2 \gamma g_{co_2}}{k_1} \right) P \\
 &= - \left( R_{\text{esp}} + \frac{\sigma_1^2}{2} \right) (\mathcal{R}_0^H - 1) + \left( b_4 + \frac{b_3 \alpha}{k_2} + \frac{b_2 q \alpha_2 \gamma g_{co_2}}{k_1} \right) P.
 \end{aligned}
 \tag{3.6}$$

Let  $f_1(W) = \frac{c\alpha_2 g_{co_2} W}{W+k_1}$  and  $f_2(P) = \frac{\alpha(P+k_2 w_0)}{P+k_2}$ , it can be noticed that  $f_2(P)$  is monotonically increasing function defined on  $[0, \infty)$ . Thus,  $f_2(P) \geq f_2(0) = \alpha w_0$ . By defining  $\beta_1 = (R_{\text{esp}} \wedge r_w \wedge \frac{\alpha w_0}{2})$  and  $\beta_2 = 1 \wedge (\frac{c}{q})^{\theta+1}$ , we combine the Itô's formula and (3.1) to obtain

$$\begin{aligned}
 \mathcal{L}V_2 &= \left( P + \frac{cW}{q\gamma} + \frac{2cS}{q\gamma} \right)^\theta \left\{ [f_1(W)P - R_{\text{esp}}P] \right. \\
 &\quad + \frac{c}{q\gamma} \left[ f_2(P)S - \frac{q\gamma}{c} f_1(W)P - r_w W \right] + \frac{2c}{q\gamma} [R - f_2(P)S] \left. \right\} \\
 &\quad + \frac{\theta}{2} \left( P + \frac{cW}{q\gamma} + \frac{2cS}{q\gamma} \right)^{\theta-1} \left( \sigma_1^2 P^2 + \frac{c^2 \sigma_2^2}{q^2 \gamma^2} W^2 + \frac{4c^2 \sigma_3^2}{q^2 \gamma^2} S^2 \right) \\
 &\leq \left( P + \frac{cW}{q\gamma} + \frac{2cS}{q\gamma} \right)^\theta \left[ \frac{2cR}{q\gamma} - R_{\text{esp}}P - \frac{cr_w W}{q\gamma} \right. \\
 &\quad \left. - \frac{c\alpha w_0}{q\gamma} S \right] + \frac{\theta}{2} (\sigma_1^2 \vee \sigma_2^2 \vee \sigma_3^2) \left( P + \frac{cW}{q\gamma} + \frac{2cS}{q\gamma} \right)^{\theta+1} \\
 &\leq \left( P + \frac{cW}{q\gamma} + \frac{2cS}{q\gamma} \right)^\theta \left[ \frac{2cR}{q\gamma} \right. \\
 &\quad \left. - \beta_1 \left( P + \frac{cW}{q\gamma} + \frac{2cS}{q\gamma} \right) \right] + \frac{\theta}{2} (\sigma_1^2 \vee \sigma_2^2 \vee \sigma_3^2) \left( P + \frac{cW}{q\gamma} + \frac{2cS}{q\gamma} \right)^{\theta+1} \\
 &\leq \Theta_0 - \frac{\beta_0}{2} \left( P + \frac{cW}{q\gamma} + \frac{2cS}{q\gamma} \right)^{\theta+1} \\
 &\leq \Theta_0 - \frac{\beta_0 \beta_2}{2} (P^{\theta+1} + W^{\theta+1} + S^{\theta+1}),
 \end{aligned}
 \tag{3.7}$$

where

$$\Theta_0 := \sup_{(P, W, S) \in \mathbb{R}_+^3} \left\{ \frac{2cR}{q\gamma} \left( P + \frac{cW}{q\gamma} + \frac{2cS}{q\gamma} \right)^\theta - \frac{\beta_0}{2} \left( P + \frac{cW}{q\gamma} + \frac{2cS}{q\gamma} \right)^{\theta+1} \right\} < \infty.$$

We choose  $M_0 > 0$ , which satisfies the condition  $M_0 \geq \frac{2(\Theta_0+r_w+\alpha w_0)+\sigma_2^2+\sigma_3^2+4}{(2R_{\text{esp}}+\sigma_1^2)(\mathcal{R}_0^H-1)}$ . That is,

$$-M_0 \left( R_{\text{esp}} + \frac{\sigma_1^2}{2} \right) (\mathcal{R}_0^H - 1) + \Theta_0 + r_w + \alpha w_0 + \frac{\sigma_2^2 + \sigma_3^2}{2} \leq -2. \tag{3.8}$$

According to (3.2)–(3.3) and (3.6)–(3.8), we then obtain that

$$\begin{aligned} \mathcal{L}V &\leq -M_0 \left( R_{\text{esp}} + \frac{\sigma_1^2}{2} \right) (\mathcal{R}_0^H - 1) + M_0 \left( b_4 + \frac{b_3\alpha}{k_2} + \frac{b_2q\alpha_2\gamma g_{\text{co}_2}}{k_1} \right) P \\ &\quad + \Theta_0 - \frac{\beta_0\beta_2}{2} (P^{\theta+1} + W^{\theta+1} + S^{\theta+1}) \\ &\quad - \frac{\alpha k_2 w_0 S}{(P + k_2)W} + \frac{q\alpha_2\gamma g_{\text{co}_2}}{k_1} P + r_w + \frac{\sigma_2^2}{2} - \frac{R}{S} + \alpha w_0 + \frac{\sigma_3^2}{2} + \frac{\alpha}{k_2} P \\ &\leq -2 - \frac{\alpha k_2 w_0 S}{(P + k_2)W} - \frac{R}{S} + \beta_3 P - \frac{\beta_0\beta_2}{2} (P^{\theta+1} + W^{\theta+1} + S^{\theta+1}), \end{aligned} \tag{3.9}$$

where  $\beta_3 := M_0 \left( b_4 + \frac{b_3\alpha}{k_2} + \frac{b_2q\alpha_2\gamma g_{\text{co}_2}}{k_1} \right) + \frac{q\alpha_2\gamma g_{\text{co}_2}}{k_1} + \frac{\alpha}{k_2} > 0$ .

**Step 2.** We define the bounded closed set

$$\mathbb{G}_\epsilon = \left\{ Q(t) \in \mathbb{R}_+^3 \mid P(t) \in \left[ \epsilon, \frac{1}{\epsilon} \right], W(t) \in \left[ \epsilon^3, \frac{1}{\epsilon^3} \right], S(t) \in \left[ \epsilon, \frac{1}{\epsilon} \right] \right\},$$

where  $\epsilon \in (0, 1)$  is a sufficiently small constant satisfying the following inequalities:

$$-2 + \Theta_1 - \frac{\beta_0\beta_2}{4} \left( \frac{1}{\epsilon} \right)^{\theta+1} \leq -1, \tag{3.10}$$

$$-2 + \Theta_1 - \frac{\beta_0\beta_2}{2} \left( \frac{1}{\epsilon} \right)^{3(\theta+1)} \leq -1, \tag{3.11}$$

$$-2 + \beta_3\epsilon \leq -1, \tag{3.12}$$

$$-2 + \Theta_1 - \frac{R \wedge (\alpha k_2 w_0)}{(1 + k_2\epsilon)\epsilon} \leq -1, \tag{3.13}$$

where  $\Theta_1 = \sup_{P \in \mathbb{R}_+^1} \{ \beta_3 P - \frac{\beta_0\beta_2}{4} P^{\theta+1} \} < \infty$ .

Next, we need to divide  $\mathbb{R}_+^3 \setminus \mathbb{G}_\epsilon$  into the following six subsets:

$$\mathbb{G}_{1,\epsilon} = \left\{ Q(t) \in \mathbb{R}_+^3 \mid P > \frac{1}{\epsilon} \right\},$$

$$\begin{aligned} \mathbb{G}_{2,\epsilon} &= \left\{ Q(t) \in \mathbb{R}_+^3 \mid S > \frac{1}{\epsilon} \right\}, \quad \mathbb{G}_{3,\epsilon} = \left\{ Q(t) \in \mathbb{R}_+^3 \mid W > \frac{1}{\epsilon^3} \right\}, \\ \mathbb{G}_{4,\epsilon} &= \left\{ Q(t) \in \mathbb{R}_+^3 \mid P < \epsilon \right\}, \\ \mathbb{G}_{5,\epsilon} &= \left\{ Q(t) \in \mathbb{R}_+^3 \mid S < \epsilon \right\}, \quad \mathbb{G}_{6,\epsilon} = \left\{ Q(t) \in \mathbb{R}_+^3 \mid W < \epsilon^3, S \geq \epsilon, P \leq \frac{1}{\epsilon} \right\}. \end{aligned}$$

Clearly,  $\mathbb{R}_+^3 \setminus \mathbb{G}_\epsilon = \bigcup_{l=1}^6 \mathbb{G}_{l,\epsilon}$ . Below we verify that  $\mathcal{L}V(Q(t)) \leq -1$  for any  $Q(t) \in \mathbb{R}_+^3 \setminus \mathbb{G}_\epsilon$ , the relevant proof can be divided into five cases.

Case 1. If  $Q(t) \in \bigcup_{i=1}^2 \mathbb{G}_{i,\epsilon}$ , combining (3.9)–(3.10), we have

$$\begin{aligned} \mathcal{L}V &\leq -2 + \left( \beta_3 P - \frac{\beta_0 \beta_2}{4} P^{\theta+1} \right) - \frac{\beta_0 \beta_2}{4} (P^{\theta+1} + S^{\theta+1}) \\ &\leq -2 + \Theta_1 - \frac{\beta_0 \beta_2}{4} \left( \frac{1}{\epsilon} \right)^{\theta+1} \leq -1. \end{aligned}$$

Case 2. If  $Q(t) \in \mathbb{G}_{3,\epsilon}$ , by (3.9) and (3.11), we have

$$\begin{aligned} \mathcal{L}V &\leq -2 + \left( \beta_3 P - \frac{\beta_0 \beta_2}{4} P^{\theta+1} \right) - \frac{\beta_0 \beta_2}{2} W^{\theta+1} \\ &\leq -2 + \Theta_1 - \frac{\beta_0 \beta_2}{2} \left( \frac{1}{\epsilon} \right)^{3(\theta+1)} \leq -1. \end{aligned}$$

Case 3. If  $Q(t) \in \mathbb{G}_{4,\epsilon}$ , by (3.9) and (3.12), we obtain

$$\mathcal{L}V \leq -2 + \beta_3 P \leq -2 + \beta_3 \epsilon \leq -1.$$

Case 4. If  $Q(t) \in \mathbb{G}_{5,\epsilon}$ , combining (3.9) and (3.13), we obtain

$$\begin{aligned} \mathcal{L}V &\leq -2 - \frac{R}{S} + \left( \beta_3 P - \frac{\beta_0 \beta_2}{4} P^{\theta+1} \right) \leq -2 + \Theta_1 - \frac{R}{\epsilon} \\ &\leq -2 + \Theta_1 - \frac{R \wedge (\alpha k_2 w_0)}{(1 + k_2 \epsilon) \epsilon} \leq -1. \end{aligned}$$

Case 5. If  $Q(t) \in \mathbb{G}_{6,\epsilon}$ , in view of (3.9) and (3.13), we obtain

$$\begin{aligned} \mathcal{L}V &\leq -2 + \Theta_1 - \frac{\alpha k_2 w_0 S}{(P + k_2) W} \leq -2 + \Theta_1 - \frac{\alpha k_2 w_0 \epsilon}{\left( \frac{1}{\epsilon} + k_2 \right) \epsilon^3} \\ &\leq -2 + \Theta_1 - \frac{R \wedge (\alpha k_2 w_0)}{(1 + k_2 \epsilon) \epsilon} \leq -1. \end{aligned}$$

In summary, for a sufficiently small  $\epsilon$  satisfying the inequalities (3.10)–(3.13), we determine that

$$\mathcal{L}V(Q(t)) \leq -1, \quad \forall Q(t) \in \mathbb{R}_+^3 \setminus \mathbb{G}_\epsilon.$$

This implies that the condition  $(\mathcal{A}_1)$  in Lemma 2.2 holds when  $\mathcal{R}_0^H > 1$ .

**Step 3.** For any given  $Q(t) \in \mathbb{G}_\epsilon$ , the diffusion matrix of system (1.2) is as follows:

$$F_0(Q(t)) = \begin{pmatrix} \sigma_1^2 P^2 & 0 & 0 \\ 0 & \sigma_2^2 W^2 & 0 \\ 0 & 0 & \sigma_3^2 S^2 \end{pmatrix} := (\psi_{ij})_{3 \times 3}.$$

Obviously,  $F_0(Q(t)) > \mathbf{0}$  for any  $t \geq 0$ , which means that the smallest eigenvalue of  $F_0(Q(t))$  is bounded away from zero. Thus, we can determine a positive number  $K_0 := \inf_{Q(t) \in \mathbb{G}_\epsilon} \{\sigma_1^2 P^2 \wedge \sigma_2^2 W^2 \wedge \sigma_3^2 S^2\}$  satisfying

$$\begin{aligned} \sum_{i=1}^3 \sum_{j=1}^3 \psi_{ij} \zeta_i \zeta_j &= \sigma_1^2 P^2 \zeta_1^2 + \sigma_2^2 W^2 \zeta_2^2 \\ &+ \sigma_3^2 S^2 \zeta_3^2 \geq K_0 \|\zeta\|^2, \quad \forall Q(t) \in \mathbb{G}_\epsilon, \zeta = (\zeta_1, \zeta_2, \zeta_3) \in \mathbb{R}^3. \end{aligned}$$

Thus, the condition  $(\mathcal{A}_2)$  in Lemma 2.2 is verified.

According to the above three steps, if  $\mathcal{R}_0^H > 1$ , the solution  $Q(t)$  is ergodic and has a unique stationary distribution  $\varpi(\cdot)$ . This completes the proof of Theorem 3.1.  $\square$

**Remark 3.1** Clearly,  $\mathcal{R}_0^S \leq \mathcal{R}_0$ , and the sign holds if and only if  $\sigma_1 = \sigma_2 = \sigma_3 = 0$ . As shown before in Section 1, by Theorems 3.1 and the local stability of the positive equilibrium  $D^*$  (i.e., Theorem A.2),  $\mathcal{R}_0^S$  can be regarded as the unified critical value for determining the persistence of vegetation of systems (1.1) and (1.2).

### 4 Probability Density Function

By Theorem 3.1, we obtain that the solution  $Q(t)$  has an ergodic stationary distribution  $\varpi(\cdot)$  if  $\mathcal{R}_0^H > 1$ . In this section, we will employ the similar method as in Zhou et al. (2021), Han et al. (2020) to study the approximate expression of the probability density function of the stationary distribution  $\varpi(\cdot)$ . Before this, we define

$$\begin{aligned} \mathcal{R}_0^C &= \frac{c\alpha_2 g_{\text{CO}_2} \alpha w_0 R}{[\alpha w_0 R + k_1(r_w + \frac{\sigma_2^2}{2})(\alpha w_0 + \frac{\sigma_3^2}{2})](R_{\text{esp}} + \frac{\sigma_1^2}{2})}, \\ \mathcal{R}_1^C &= \frac{q\gamma k_2(R_{\text{esp}} + \frac{\sigma_1^2}{2})(\alpha w_0 + \frac{\sigma_3^2}{2})^2}{c\alpha R(1 - w_0)} - \frac{\sigma_3^2}{2}. \end{aligned}$$

Moreover, two main transformations of system (1.2) should be first presented.

### 4.1 Logarithmic Transformation of System (1.2)

Let  $z_1 = \ln P$ ,  $z_2 = \ln W$  and  $z_3 = \ln S$ . Applying the Itô's formula to  $z_i, i = 1, 2, 3$ , we have

$$\begin{cases} dz_1 = \left[ \frac{c\alpha_2 g_{co_2} e^{z_2}}{e^{z_2} + k_1} - \left( R_{esp} + \frac{\sigma_1^2}{2} \right) \right] dt + \sigma_1 dB_1(t), \\ dz_2 = \left[ \frac{\alpha(e^{z_1} + k_2 w_0) e^{z_3 - z_2}}{e^{z_1} + k_2} - \frac{q\alpha_2 \gamma g_{co_2} e^{z_1}}{e^{z_2} + k_1} - \left( r_w + \frac{\sigma_2^2}{2} \right) \right] dt + \sigma_2 dB_2(t), \\ dz_3 = \left[ R e^{-z_3} - \frac{\alpha(e^{z_1} + k_2 w_0)}{e^{z_1} + k_2} - \frac{\sigma_3^2}{2} \right] dt + \sigma_3 dB_3(t). \end{cases} \tag{4.1}$$

Similar to the vegetation-positive equilibrium  $D^*$  of deterministic system (1.1), we define a quasi-positive equilibrium  $\bar{D}^* = (\bar{P}^*, \bar{W}^*, \bar{S}^*)^T$ , which satisfies the following:

$$\begin{cases} \frac{c\alpha_2 g_{co_2} \bar{W}^*}{\bar{W}^* + k_1} - \left( R_{esp} + \frac{\sigma_1^2}{2} \right) = 0, \\ \frac{\alpha(\bar{P}^* + k_2 w_0) \bar{S}^*}{(\bar{P}^* + k_2) \bar{W}^*} - \frac{q\alpha_2 \gamma g_{co_2} \bar{P}^*}{\bar{W}^* + k_1} - \left( r_w + \frac{\sigma_2^2}{2} \right) = 0, \\ \frac{R}{\bar{S}^*} - \frac{\alpha(\bar{P}^* + k_2 w_0)}{\bar{P}^* + k_2} - \frac{\sigma_3^2}{2} = 0. \end{cases} \tag{4.2}$$

By direct calculation, we obtain that  $\bar{W}^* = \frac{k_1(R_{esp} + \frac{\sigma_1^2}{2})}{c\alpha_2 g_{co_2} - (R_{esp} + \frac{\sigma_1^2}{2})}$ ,  $\bar{S}^* = \frac{2R(\bar{P}^* + k_2)}{(2\alpha + \sigma_3^2)\bar{P}^* + k_2(2\alpha w_0 + \sigma_3^2)}$ , and  $\bar{P}^*$  is the root of the nonlinear equation

$$\begin{aligned} R - \frac{k_1(r_w + \frac{\sigma_2^2}{2})(R_{esp} + \frac{\sigma_1^2}{2})}{c\alpha_2 g_{co_2} - (R_{esp} + \frac{\sigma_1^2}{2})} &= \frac{q\gamma(R_{esp} + \frac{\sigma_1^2}{2})\bar{P}^*}{c} \\ &+ \frac{\sigma_3^2 R(\bar{P}^* + k_2)}{(2\alpha + \sigma_3^2)\bar{P}^* + k_2(2\alpha w_0 + \sigma_3^2)}. \end{aligned} \tag{4.3}$$

Let  $F(p) := \frac{q\gamma(R_{esp} + \frac{\sigma_1^2}{2})p}{c} + \frac{\sigma_3^2 R(p + k_2)}{(2\alpha + \sigma_3^2)p + k_2(2\alpha w_0 + \sigma_3^2)}$ , where  $p \geq 0$ . If  $\mathcal{R}_1^C \geq 0$ , we have

$$\begin{aligned} F'(p) &= \frac{q\gamma(R_{esp} + \frac{\sigma_1^2}{2})}{c} - \frac{2\alpha\sigma_3^2 Rk_2(1 - w_0)}{[(2\alpha + \sigma_3^2)p + k_2(2\alpha w_0 + \sigma_3^2)]^2} \\ &\geq \frac{q\gamma(R_{esp} + \frac{\sigma_1^2}{2})}{c} - \frac{2\alpha\sigma_3^2 R(1 - w_0)}{k_2(2\alpha w_0 + \sigma_3^2)^2} = \frac{4\alpha R(1 - w_0)\mathcal{R}_1^C}{k_2(2\alpha w_0 + \sigma_3^2)^2} \geq 0. \end{aligned}$$



This implies that  $F(p)$  is a monotonically increasing function on  $[0, \infty)$ . Thus, Eq. (4.3) has at most one positive root. Clearly,  $\mathcal{R}_0^H \leq \mathcal{R}_0^C \leq \mathcal{R}_0$ , which means that  $\mathcal{R}_0^C > 1$  if  $\mathcal{R}_0^H > 1$ . Moreover, if  $\mathcal{R}_0^H > 1$ , we easily obtain that  $c\alpha_2 g_{co_2} > (R_{\text{esp}} + \frac{\sigma_1^2}{2})$ ,

$$\begin{aligned} \text{(i)} \quad & R - \frac{k_1(r_w + \frac{\sigma_2^2}{2})(R_{\text{esp}} + \frac{\sigma_1^2}{2})}{c\alpha_2 g_{co_2} - (R_{\text{esp}} + \frac{\sigma_1^2}{2})} - F(0) \\ &= \frac{[\alpha w_0 R + k_1(r_w + \frac{\sigma_2^2}{2})(\alpha w_0 + \frac{\sigma_3^2}{2})](R_{\text{esp}} + \frac{\sigma_1^2}{2})}{(\alpha w_0 + \frac{\sigma_2^2}{2})[c\alpha_2 g_{co_2} - (R_{\text{esp}} + \frac{\sigma_1^2}{2})]} (\mathcal{R}_0^C - 1) > 0, \end{aligned}$$

and (ii)  $R - \frac{k_1(r_w + \frac{\sigma_2^2}{2})(R_{\text{esp}} + \frac{\sigma_1^2}{2})}{c\alpha_2 g_{co_2} - (R_{\text{esp}} + \frac{\sigma_1^2}{2})} - F(\infty) = -\infty$ .

In summary, if  $\mathcal{R}_0^H > 1$  and  $\mathcal{R}_1^C \geq 0$ , the solution of Eq. (4.3) is unique and  $\bar{D}^* \in \mathbb{R}_+^3$ . In this sense, we define  $\bar{D}^* = (e^{z_1^*}, e^{z_2^*}, e^{z_3^*})^T$ , i.e.,  $z_1^* = \ln \bar{P}^*$ ,  $z_2^* = \ln \bar{W}^*$  and  $z_3^* = \ln \bar{S}^*$ .

If there is no environmental noise,  $\bar{D}^*$  coincides with  $D^*$  in deterministic system (1.1). In addition, the conditions  $\mathcal{R}_0^H > 1$  and  $\mathcal{R}_1^C \geq 0$  are equivalent to  $\mathcal{R}_0 > 1$ . Thus,  $\bar{D}^*$  and  $\mathcal{R}_1^C \geq 0$  are biologically reasonable assumptions involved in the stochasticity.

### 4.2 Linearized Transformation of System (4.1)

We define  $B(t) = (B_1(t), B_2(t), B_3(t))^T$  and  $X(t) = (x_1, x_2, x_3)^T$ , where  $x_i = z_i - z_i^*$ ,  $i = 1, 2, 3$ . Then, the linearized equation of system (4.1) around the equilibrium  $(z_1^*, z_2^*, z_3^*)^T$  is as follows:

$$\begin{aligned} dX(t) &= \begin{pmatrix} 0 & a_{12} & 0 \\ -a_{21} & -a_{22} & a_{23} \\ -a_{31} & 0 & -a_{33} \end{pmatrix} X(t)dt + \begin{pmatrix} \sigma_1 & 0 & 0 \\ 0 & \sigma_2 & 0 \\ 0 & 0 & \sigma_3 \end{pmatrix} dB(t) \\ &:= A_0 X(t)dt + \Lambda dB(t), \end{aligned} \tag{4.4}$$

where  $a_{12} = \frac{c\alpha_2 g_{co_2} k_1 \bar{W}^*}{(\bar{W}^* + k_1)^2} > 0$ ,  $a_{21} = \frac{q\alpha_2 \gamma g_{co_2} \bar{P}^*}{\bar{W}^* + k_1} - \frac{\alpha k_2 (1 - w_0) \bar{P}^* \bar{S}^*}{(\bar{P}^* + k_2)^2 \bar{W}^*}$ ,  $a_{22} = \frac{\alpha(\bar{P}^* + k_2 w_0) \bar{S}^*}{(\bar{P}^* + k_2) \bar{W}^*} - \frac{q\alpha_2 \gamma g_{co_2} \bar{P}^* \bar{W}^*}{(\bar{W}^* + k_1)^2}$ ,  $a_{23} = \frac{\alpha(\bar{P}^* + k_2 w_0) \bar{S}^*}{(\bar{P}^* + k_2) \bar{W}^*} > 0$ ,  $a_{31} = \frac{\alpha k_2 (1 - w_0) \bar{P}^*}{(\bar{P}^* + k_2)^2} > 0$  and  $a_{33} = \frac{R}{\bar{S}^*} > 0$ .

### 4.3 Local Density Function of Stationary Distribution $\varpi(\cdot)$

By the theory of Gardiner (1983), for any time  $t$ , the transient density function  $\Psi(X(t), t)$  of the solution  $X(t)$  of system (4.4) is determined by the following Fokker–

Planck equation Jordan et al. (1998):

$$\frac{\partial \Psi(X(t), t)}{\partial t} = - \sum_{j=1}^3 \frac{\partial}{\partial x_j} [A_0^{(j)} X(t) \Psi(X(t), t)] + \sum_{j=1}^3 \frac{\sigma_j^2}{2} \frac{\partial^2 \Psi(X(t), t)}{\partial x_j^2}, \tag{4.5}$$

where  $A_0^{(i)}$  denotes the  $i$ th row vector of  $A_0$ ,  $i = 1, 2, 3$ . By the standard argument of Mao (1997) and Roozen (1989), system (4.4) with the initial value  $X(0)$  has a unique explicit solution  $X(t) = e^{A_0 t} X(0) + \int_0^t e^{A_0(t-\varsigma)} \Lambda dB(\varsigma)$ . Note that  $\Lambda$  is a constant matrix, thus  $\int_0^t e^{A_0(t-\varsigma)} \Lambda dB(\varsigma)$  follows a Gaussian distribution, implying that system (4.4) has a unique invariant (or stationary) Gaussian distribution  $\mathbb{F}(\cdot)$  and the distribution of the solution  $X(t)$  will approach  $\mathbb{F}(\cdot)$  as  $t \rightarrow \infty$ . For simplicity, let  $\Psi^*(X(t)) = \chi_0 e^{-\frac{1}{2} X^T L X}$  be the density function of  $\mathbb{F}(\cdot)$ , where  $\chi_0$  satisfies the normalization condition and  $L$  is a real symmetric matrix. In this sense, the transient density function  $\Psi(X(t), t)$  will converge to the invariant density function  $\Psi^*(X(t))$ , that is,  $\lim_{t \rightarrow \infty} \int_{\mathbb{R}^3} |\Psi(X(t), t) - \Psi^*(X(t))| dX = 0$  (Liu et al. 2020; Lin and Jiang 2014). Combining  $\frac{\partial \Psi^*(X(t))}{\partial t} = 0$  and Eq. (4.5), the invariant density function  $\Psi^*(X(t))$  satisfies the following equation:

$$\begin{aligned} & - \sum_{j=1}^3 \frac{\sigma_j^2}{2} \frac{\partial^2 \Psi^*}{\partial x_j^2} + \frac{\partial}{\partial x_1} (a_{12} x_2 \Psi^*) + \frac{\partial}{\partial x_2} [(-a_{21} x_1 - a_{22} x_2 + a_{23} x_3) \Psi^*] \\ & + \frac{\partial}{\partial x_3} [(-a_{31} x_1 - a_{33} x_3) \Psi^*] = 0. \end{aligned} \tag{4.6}$$

Substituting the expression of  $\Psi^*(X(t))$  into Eq. (4.6),  $L$  satisfies the following real algebraic equation:

$$L A^2 L + L A_0 + A_0^T L = 0.$$

We consider the following auxiliary algebraic equation:

$$A^2 + A_0 \Sigma + \Sigma A_0^T = 0. \tag{4.7}$$

If we can prove that  $\Sigma$  in (4.7) is unique and positive definite, then  $L = \Sigma^{-1} \succ \mathbf{0}$ . By Lemma 2.1, we determine that  $A_0 \in \overline{RH}(3)$  is the necessary condition for  $\Sigma \succ \mathbf{0}$ . By direct calculation, we have

$$\phi_{A_0}(y) = y^3 + \lambda_1 y^2 + \lambda_2 y + \lambda_3,$$

where  $\lambda_1 = a_{22} + a_{33}$ ,  $\lambda_2 = a_{22} a_{33} + a_{12} a_{21}$  and  $\lambda_3 = a_{12} (a_{23} a_{31} + a_{21} a_{33})$ . Combined with Definition 2.1, we get that  $A_0 \in \overline{RH}(3)$  if and only if  $\lambda_1 > 0$ ,  $\lambda_3 > 0$  and  $\lambda_1 \lambda_2 - \lambda_3 > 0$ . In view of the second equality of Eq. (4.2), one can see that

$$a_{22} \geq \frac{\alpha(\overline{P}^* + k_2 w_0) \overline{S}^*}{(\overline{P}^* + k_2) \overline{W}^*}$$

$$-\frac{q\alpha_2\gamma g_{\text{CO}_2} \bar{P}^*}{\bar{W}^* + k_1} = r_w + \frac{\sigma_2^2}{2} > 0,$$

which implies that  $\lambda_1 = a_{22} + a_{33} > 0$ . We consider the following necessary assumption:

**Assumption 4.1**  $\mathcal{R}_1^C \geq 0, \lambda_3 > 0$  and  $\lambda_1\lambda_2 - \lambda_3 > 0$ .

It is evident that  $A_0 \in \overline{RH}(3)$  if Assumption 4.1 holds. Moreover, we define an important critical value by  $\Delta = \frac{a_{23}a_{31} + a_{21}(a_{33} - a_{22})}{a_{31}}$ .

**Theorem 4.1** Under Assumption 4.1, if  $\mathcal{R}_0^H > 1$ , then the stationary distribution  $\varpi(\cdot)$  around the equilibrium  $\bar{D}^*$  approximately has a log-normal probability density function  $\Upsilon(P, W, S)$  which take form of

$$\Upsilon(P, W, S) = (2\pi)^{-\frac{3}{2}} |\Sigma|^{-\frac{1}{2}} (PWS)^{-1} e^{-\frac{1}{2} (\ln \frac{P}{P^*}, \ln \frac{W}{W^*}, \ln \frac{S}{S^*}) \Sigma^{-1} (\ln \frac{P}{P^*}, \ln \frac{W}{W^*}, \ln \frac{S}{S^*})^T}, \tag{4.8}$$

where  $\Sigma > \mathbf{0}$ , and the special form of  $\Sigma$  is given as follows.

(i) If  $\Delta = 0$ , then

$$\Sigma = \delta_1 (J_1 H_1)^{-1} \Pi_1 [(J_1 H_1)^{-1}]^T + \delta_2 (J_2 H_2)^{-1} \Pi_0 [(J_2 H_2)^{-1}]^T + \delta_3 (J_3 H_3)^{-1} \Pi_0 [(J_3 H_3)^{-1}]^T,$$

(ii) If  $\Delta \neq 0$ , then

$$\Sigma = \delta_1 \Delta^2 (\hat{J}_1 H_1)^{-1} \Pi_0 [(\hat{J}_1 H_1)^{-1}]^T + \delta_2 (J_2 H_2)^{-1} \Pi_0 [(J_2 H_2)^{-1}]^T + \delta_3 (J_3 H_3)^{-1} \Pi_0 [(J_3 H_3)^{-1}]^T$$

with

$$H_1 = \begin{pmatrix} 1 & 0 & 0 \\ 0 & 0 & 1 \\ 0 & 1 & -\frac{a_{21}}{a_{31}} \end{pmatrix}, \quad \Pi_0 = \begin{pmatrix} \frac{\lambda_2}{2(\lambda_1\lambda_2 - \lambda_3)} & 0 & -\frac{1}{2(\lambda_1\lambda_2 - \lambda_3)} \\ 0 & \frac{1}{2(\lambda_1\lambda_2 - \lambda_3)} & 0 \\ -\frac{1}{2(\lambda_1\lambda_2 - \lambda_3)} & 0 & \frac{\lambda_1}{2\lambda_3(\lambda_1\lambda_2 - \lambda_3)} \end{pmatrix},$$

$$\Pi_1 = \begin{pmatrix} \frac{1}{2a_{33}} & 0 & 0 \\ 0 & \frac{1}{2a_{12}a_{21}a_{33}} & 0 \\ 0 & 0 & 0 \end{pmatrix},$$

$$H_2 = \begin{pmatrix} 0 & 1 & 0 \\ 1 & 0 & 0 \\ 0 & 0 & 1 \end{pmatrix}, \quad H_3 = \begin{pmatrix} 0 & 0 & 1 \\ 0 & 1 & 0 \\ 1 & 0 & 0 \end{pmatrix},$$

$$\hat{J}_1 = \begin{pmatrix} -a_{31}\Delta & -(a_{22} + a_{33})\Delta & a_{22}^2 \\ 0 & \Delta & -a_{22} \\ 0 & 0 & 1 \end{pmatrix},$$

$$J_1 = \begin{pmatrix} -a_{31} & -a_{33} & 0 \\ 0 & 1 & 0 \\ 0 & 0 & 1 \end{pmatrix}, J_2 = \begin{pmatrix} -a_{12}a_{31} & a_{31}a_{33} & a_{33}^2 \\ 0 & -a_{31} & -a_{33} \\ 0 & 0 & 1 \end{pmatrix},$$

$$J_3 = \begin{pmatrix} a_{12}a_{23} & -a_{12}a_{22} & -a_{12}a_{21} \\ 0 & a_{12} & 0 \\ 0 & 0 & 1 \end{pmatrix}$$

and  $\delta_1 = (a_{31}\sigma_1)^2, \delta_2 = (a_{12}a_{31}\sigma_2)^2, \delta_3 = (a_{12}a_{23}\sigma_3)^2$ .

**Proof** Note that  $\Lambda^2 = \text{diag}\{\sigma_1^2, \sigma_2^2, \sigma_3^2\}$ , where  $\sigma_i^2 > 0 (\forall i = 1, 2, 3)$ . Combined with Lemma 2.1, we obtain that  $\Sigma$  is unique and positive definite under Assumption 4.1, implying that  $L > \mathbf{0}$ . Thus, we compute that  $\chi_0 = (2\pi)^{-\frac{3}{2}}|\Sigma|^{-\frac{1}{2}}$ . Moreover, the solution  $X(t)$  of system (4.4) has a stationary normal distribution  $\mathbb{F}(\cdot)$ . By Theorem 3.1, the solution  $(P(t), W(t), S(t))^T$  of system (1.2) has a unique stationary distribution  $\varpi(\cdot)$  when  $\mathcal{R}_0^H > 1$ . In view of the transformation  $X(t) = (\ln \frac{P(t)}{P^*}, \ln \frac{W(t)}{W^*}, \ln \frac{S(t)}{S^*})^T$  and the relationship between systems (1.2) and (4.4), we determine that the stationary distribution  $\varpi(\cdot)$  around the equilibrium  $\overline{D}^*$  can be approximated by a log-normal distribution. That is to say, the stationary distribution  $\varpi(\cdot)$  around the equilibrium  $\overline{D}^*$  approximately has a log-normal density function  $\Upsilon(P, W, S)$  and it is

$$\Upsilon(P, W, S) = (2\pi)^{-\frac{3}{2}}|\Sigma|^{-\frac{1}{2}}(PWS)^{-1}e^{-\frac{1}{2}(\ln \frac{P}{P^*}, \ln \frac{W}{W^*}, \ln \frac{S}{S^*})\Sigma^{-1}(\ln \frac{P}{P^*}, \ln \frac{W}{W^*}, \ln \frac{S}{S^*})^T}.$$

To prove Theorem 4.1, we only need to obtain the explicit form of  $\Sigma$  in Eq. (4.7). Using the finite independent superposition principle, let  $\Sigma_i (i = 1, 2, 3)$  be the solutions of the following algebraic equations, respectively:

$$\Lambda_j + A_0\Sigma_j + \Sigma_j A_0^T = 0,$$

where  $\Lambda_1 = \text{diag}\{1, 0, 0\}, \Lambda_2 = \text{diag}\{0, 1, 0\}$  and  $\Lambda_3 = \text{diag}\{0, 0, 1\}$ . Obviously,  $\Sigma = \sigma_1^2\Sigma_1 + \sigma_2^2\Sigma_2 + \sigma_3^2\Sigma_3$ . The explicit form of  $\Sigma$  is derived by the following three steps.

**Step 1.** Consider the algebraic equation

$$\Lambda_1 + A_0\Sigma_1 + \Sigma_1 A_0^T = 0. \tag{4.9}$$

For the following first elimination matrix  $H_1$ , by letting  $C_1 = H_1 A_0 H_1^{-1}$ , we obtain

$$H_1 = \begin{pmatrix} 1 & 0 & 0 \\ 0 & 0 & 1 \\ 0 & 1 & -\frac{a_{21}}{a_{31}} \end{pmatrix}, C_1 = \begin{pmatrix} 0 & \frac{a_{12}a_{21}}{a_{31}} & a_{12} \\ -a_{31} & -a_{33} & 0 \\ 0 & \Delta & -a_{22} \end{pmatrix},$$

where  $\Delta$  is the same as that in Theorem 4.1. We consider the following two cases of  $\Delta$ :

$$(\mathcal{B}_1). \Delta = 0, (\mathcal{B}_2). \Delta \neq 0.$$

Case 1. If  $\Delta = 0$ , i.e.,  $a_{23}a_{31} = a_{21}(a_{22} - a_{33})$ , then  $\lambda_3 = a_{12}a_{21}a_{22}$ . By Assumption 4.1, we determine that  $a_{12}a_{21} > 0$ . Let  $\tilde{C}_1 = J_1 C_1 J_1^{-1}$ , where the standardized transformation matrix  $J_1$  and  $\tilde{C}_1$  are obtained by

$$J_1 = \begin{pmatrix} -a_{31} & -a_{33} & 0 \\ 0 & 1 & 0 \\ 0 & 0 & 1 \end{pmatrix}, \quad \tilde{C}_1 = \begin{pmatrix} -a_{33} & -a_{12}a_{21} & -a_{12}a_{31} \\ 1 & 0 & 0 \\ 0 & \Delta & -a_{22} \end{pmatrix}. \quad (4.10)$$

According to Zhou et al. (2021),  $\tilde{C}_1$  is a standard  $R_2$  matrix. In view of  $(J_1 H_1) \Lambda_1^2 (J_1 H_1)^T = a_{31}^2 \Lambda_1$ , Eq. (4.9) can then be equivalently transformed into

$$\Lambda_1 + \tilde{C}_1 \left[ \frac{1}{a_{31}^2} (J_1 H_1) \Sigma_1 (J_1 H_1)^T \right] + \left[ \frac{1}{a_{31}^2} (J_1 H_1) \Sigma_1 (J_1 H_1)^T \right] \tilde{C}_1^T = 0.$$

Using Lemma 5 of Han et al. (2020), we obtain

$$\frac{1}{a_{31}^2} (J_1 H_1) \Sigma_1 (J_1 H_1)^T = \Pi_1 = \begin{pmatrix} \frac{1}{2a_{33}} & 0 & 0 \\ 0 & \frac{1}{2a_{12}a_{21}a_{33}} & 0 \\ 0 & 0 & 0 \end{pmatrix} \geq \mathbf{0}. \quad (4.11)$$

Thus,  $\Sigma_1 = a_{31}^2 (J_1 H_1)^{-1} \Pi_1 [(J_1 H_1)^{-1}]^T \geq \mathbf{0}$ .

Case 2. If  $\Delta \neq 0$ , we define  $\hat{C}_1 = \hat{J}_1 C_1 \hat{J}_1^{-1}$ , where  $\hat{C}_1$  and the new standardized transformation matrix  $\hat{J}_1$  are derived by

$$\hat{J}_1 = \begin{pmatrix} -a_{31}\Delta & -(a_{22} + a_{33})\Delta & a_{22}^2 \\ 0 & \Delta & -a_{22} \\ 0 & 0 & 1 \end{pmatrix}, \quad \hat{C}_1 = \begin{pmatrix} -\lambda_1 & -\lambda_2 & -\lambda_3 \\ 0 & 1 & 0 \\ 0 & 0 & 1 \end{pmatrix}, \quad (4.12)$$

where  $\lambda_i$  ( $i = 1, 2, 3$ ) are the same as those in Theorem 4.1. By Han et al. (2020),  $\hat{C}_1$  is a standard  $R_1$  matrix. A direct calculation shows that  $(\hat{J}_1 H_1) \Lambda_1^2 (\hat{J}_1 H_1)^T = (a_{31}\Delta)^2 \Lambda_1$ . Then, Eq. (4.9) can be equivalently transformed into

$$\Lambda_1 + \hat{C}_1 \left[ \frac{1}{(a_{31}\Delta)^2} (\hat{J}_1 H_1) \Sigma_1 (\hat{J}_1 H_1)^T \right] + \left[ \frac{1}{(a_{31}\Delta)^2} (\hat{J}_1 H_1) \Sigma_1 (\hat{J}_1 H_1)^T \right] \hat{C}_1^T = 0. \quad (4.13)$$

As shown in Lemma 2.3 of Zhou et al. (2021), we can determine that  $\frac{1}{(a_{31}\Delta)^2} (\hat{J}_1 H_1) \Sigma_1 (\hat{J}_1 H_1)^T := \Pi_0 > \mathbf{0}$  and

$$\Pi_0 = \begin{pmatrix} \frac{\lambda_2}{2(\lambda_1\lambda_2 - \lambda_3)} & 0 & -\frac{1}{2(\lambda_1\lambda_2 - \lambda_3)} \\ 0 & \frac{1}{2(\lambda_1\lambda_2 - \lambda_3)} & 0 \\ -\frac{1}{2(\lambda_1\lambda_2 - \lambda_3)} & 0 & \frac{\lambda_1}{2\lambda_3(\lambda_1\lambda_2 - \lambda_3)} \end{pmatrix}. \quad (4.14)$$

Thus,  $\Sigma_1 = (a_{21}\Delta)^2 (\hat{J}_1 H_1)^{-1} \Pi_0 [(\hat{J}_1 H_1)^{-1}]^T > \mathbf{0}$ .

**Step 2.** Consider the following algebraic equation:

$$\Lambda_2 + A_0 \Sigma_2 + \Sigma_2 A_0^T = 0. \tag{4.15}$$

Let  $C_2 = H_2 A_0 H_2^{-1}$ , where the second elimination matrix  $H_2$  and  $C_2$  are

$$H_2 = \begin{pmatrix} 0 & 1 & 0 \\ 1 & 0 & 0 \\ 0 & 0 & 1 \end{pmatrix}, \quad C_2 = \begin{pmatrix} -a_{22} & -a_{21} & a_{23} \\ a_{12} & 0 & 0 \\ 0 & -a_{31} & -a_{33} \end{pmatrix}.$$

By a method similar to that shown in Case 2 of Step 1, we construct a standardized transformation matrix  $J_2$  as follows:

$$J_2 = \begin{pmatrix} -a_{12}a_{31} & a_{31}a_{33} & a_{33}^2 \\ 0 & -a_{31} & -a_{33} \\ 0 & 0 & 1 \end{pmatrix}. \tag{4.16}$$

Let  $\tilde{C}_2 = J_2 C_2 J_2^{-1}$ , a direct calculation shows that  $\tilde{C}_2 = \hat{C}_1$ , that is,  $\tilde{C}_2$  is also a standard  $R_1$  matrix. Combined with  $(J_2 H_2) \Lambda_2 (J_2 H_2)^T = (a_{12} a_{31})^2 \Lambda_1$ , we can then transform Eq. (4.15) into

$$\Lambda_1 + \hat{C}_1 \left[ \frac{1}{(a_{12} a_{31})^2} (J_2 H_2) \Sigma_1 (J_2 H_2)^T \right] + \left[ \frac{1}{(a_{12} a_{31})^2} (J_2 H_2) \Sigma_1 (J_2 H_2)^T \right] \hat{C}_1^T = 0. \tag{4.17}$$

Combining (4.13)–(4.14), the solution of Eq. (4.17) is unique and it is

$$\frac{1}{(a_{12} a_{31})^2} (J_2 H_2) \Sigma_1 (J_2 H_2)^T = \Pi_0 > \mathbf{0}.$$

Thus,  $\Sigma_2 = (a_{12} a_{31})^2 (J_2 H_2)^{-1} \Pi_0 [(J_2 H_2)^{-1}]^T > \mathbf{0}$ .

**Step 3.** Consider the following algebraic equation:

$$\Lambda_3 + A_0 \Sigma_3 + \Sigma_3 A_0^T = 0. \tag{4.18}$$

Similarly, we define  $C_3 = (J_3 H_3) A_0 (J_3 H_3)^{-1}$ , where the third elimination  $H_3$  and standardized transformation matrix  $J_3$  are

$$H_3 = \begin{pmatrix} 0 & 0 & 1 \\ 0 & 1 & 0 \\ 1 & 0 & 0 \end{pmatrix}, \quad J_3 = \begin{pmatrix} a_{12}a_{23} & -a_{12}a_{22} & -a_{12}a_{21} \\ 0 & a_{12} & 0 \\ 0 & 0 & 1 \end{pmatrix}.$$

By direct calculation, we obtain that  $C_3 = \hat{C}_1$  and  $(J_3 H_3) \Lambda_3 (J_3 H_3)^T = (a_{12} a_{23})^2 \Lambda_1$ . Thus, Eq. (4.18) can be equivalently rewritten as

$$\Lambda_1 + \hat{C}_1 \left[ \frac{1}{(a_{12} a_{23})^2} (J_3 H_3) \Sigma_1 (J_3 H_3)^T \right] + \left[ \frac{1}{(a_{12} a_{23})^2} (J_3 H_3) \Sigma_1 (J_3 H_3)^T \right] \hat{C}_1^T = 0.$$

By Eqs. (4.13) and (4.17), we easily get that

$$\frac{1}{(a_{12}a_{23})^2} (J_3 H_3) \Sigma_1 (J_3 H_3)^T = \Pi_0,$$

implying that  $\Sigma_3 = (a_{12}a_{23})^2 (J_3 H_3)^{-1} \Pi_0 [(J_3 H_3)^{-1}]^T > \mathbf{0}$ .

According to the above three steps, the explicit form of  $\Sigma$  shown in Theorem 4.1 can be obtained by the definitions of  $\delta_i$  ( $i = 1, 2, 3$ ).

In summary, the stationary distribution  $\varpi(\cdot)$  around the equilibrium  $\bar{D}^*$  approximately has a three-dimensional log-normal density function  $\Upsilon(P, W, S)$  which shown in (4.8). This completes the proof of Theorem 4.1. □

**Remark 4.1** If  $\mathcal{R}_0^H > 1$ , Theorem 3.1 shows that all of the distributions of the subpopulations  $P(t)$ ,  $W(t)$  and  $S(t)$  will separately converge to the corresponding stationary marginal distributions  $\mu_1(P)$ ,  $\mu_2(W)$  and  $\mu_3(S)$  of  $\varpi(\cdot)$  as  $t \rightarrow \infty$ . By letting  $\Sigma = (\rho_{ij})_{3 \times 3}$ , we then combine Theorem 4.1 to obtain that the distribution  $\mu_1(P)$  around  $\bar{P}^*$  approximately has a log-normal density function  $\ell_1(P)$ . Moreover, the distribution  $\mu_2(W)$  around  $\bar{W}^*$  approximately has a log-normal density function  $\ell_2(W)$  and the distribution  $\mu_3(S)$  around  $\bar{S}^*$  approximately has a log-normal density function  $\ell_3(S)$ , where

$$\begin{aligned} \ell_1(P) &= \frac{1}{P\sqrt{2\pi\rho_{11}}} e^{-\frac{(\ln P - \ln \bar{P}^*)^2}{2\rho_{11}}}, & \ell_2(W) &= \frac{1}{W\sqrt{2\pi\rho_{22}}} e^{-\frac{(\ln W - \ln \bar{W}^*)^2}{2\rho_{22}}}, \\ \ell_3(S) &= \frac{1}{S\sqrt{2\pi\rho_{33}}} e^{-\frac{(\ln S - \ln \bar{S}^*)^2}{2\rho_{33}}}. \end{aligned}$$

### 5 Vegetation Extinction

As is well known, a major concern of ecological protection is how to prevent vegetation extinction in arid ecosystems. In this section, we will first establish sufficient conditions for the exponential extinction of vegetation of system (1.2).

**Theorem 5.1** *If  $\mathcal{R}_0^E := \frac{c\alpha_2 g_{\text{CO}_2}}{R_{\text{esp}} + \frac{\sigma_1^2}{2}} < 1$ , then the vegetation of system (1.2) will die out with probability 1, namely  $\lim_{t \rightarrow \infty} P(t) = 0$  a.s. Moreover,*

$$\limsup_{t \rightarrow \infty} \frac{\ln P(t)}{t} \leq \left( R_{\text{esp}} + \frac{\sigma_1^2}{2} \right) (\mathcal{R}_0^E - 1) < 0 \text{ a.s.}, \tag{5.1}$$

which means that the exponential decay rate of vegetation is at least  $(R_{\text{esp}} + \frac{\sigma_1^2}{2})(\mathcal{R}_0^E - 1)$  in the long term.

**Proof** Applying the Itô’s formula to  $\ln P(t)$ , we have

$$d \ln P(t) = \left[ \frac{c\alpha_2 g_{\text{CO}_2} W(t)}{W(t) + k_1} - \left( R_{\text{esp}} + \frac{\sigma_1^2}{2} \right) \right] dt + \sigma_1 dB_1(t)$$

$$\leq \left[ c\alpha_2 g_{CO_2} - \left( R_{\text{esp}} + \frac{\sigma_1^2}{2} \right) \right] dt + \sigma_1 dB_1(t). \tag{5.2}$$

Integrating from 0 to  $t$  and dividing by  $t$  on both sides of (5.2), we obtain

$$\begin{aligned} \frac{\ln P(t)}{t} - \frac{\ln P(0)}{t} &\leq \frac{1}{t} \int_0^t \left[ c\alpha_2 g_{CO_2} - \left( R_{\text{esp}} + \frac{\sigma_1^2}{2} \right) \right] d\zeta + \frac{\int_0^t \sigma_1 dB_1(\zeta)}{t} \\ &= \left( R_{\text{esp}} + \frac{\sigma_1^2}{2} \right) (\mathcal{R}_0^E - 1) + \frac{\int_0^t \sigma_1 dB_1(\zeta)}{t}. \end{aligned} \tag{5.3}$$

Using the strong law of large numbers for the local martingale (Lipster 1980), we have

$$\lim_{t \rightarrow \infty} \frac{\int_0^t \sigma_1 dB_1(\zeta)}{t} = 0 \text{ a.s.} \tag{5.4}$$

Taking the superior limit of  $t \rightarrow \infty$  on both sides of (5.3), (5.1) can then be proved by (5.4), which implies that  $\lim_{t \rightarrow \infty} P(t) = 0$  a.s. and the exponential decay rate of vegetation  $P(t)$  of system (1.2) is at least  $(R_{\text{esp}} + \frac{\sigma_1^2}{2})(\mathcal{R}_0^E - 1)$  in the long term. Thus, the proof of Theorem 5.1 is completed.  $\square$

**Remark 5.1** Clearly,  $\mathcal{R}_0^H \leq \mathcal{R}_0^E$ . By Theorems 3.1 and 5.1, we can determine that the impact of stochastic noise on long-time stability of vegetation system is generally negative. Specifically, for some stochastic noises satisfying the condition  $(\mathcal{R}_0^H \leq \mathcal{R}_0^E < 1 < \mathcal{R}_0)$ , the vegetation  $P(t)$  of deterministic system (1.1) may be persistent, but it will go to extinction in the stochastic system (1.2).

Theorem 5.1 presents a criterion  $\mathcal{R}_0^E < 1$  for the extinction of vegetation in system (1.2). However, if the average extinction time is large, then this criterion may be not useful in practice. In this sense, when  $\mathcal{R}_0^E < 1$ , we need to estimate the probability of vegetation extinction at a given time. In practical terms, we usually select a critical value  $\epsilon$  as an index of the extinction of vegetation in an arid ecosystem. That is, we think that the vegetation  $P(t)$  is extinct if  $P(t) \leq \epsilon$  for any  $t \geq t_0(\epsilon)$ .

**Theorem 5.2** For any  $\epsilon > 0$ , if  $\mathcal{R}_0^E < 1$ , then the vegetation  $P(t)$  ( $t > 0$ ) of system (1.2) follows:

$$\mathbb{P}\{P(t) \leq \epsilon\} \geq \Phi\left(\frac{\beta t + \ln \epsilon - \ln P(0)}{\sigma_1 \sqrt{t}}\right) \text{ a.s.,}$$

where  $\beta = (R_{\text{esp}} + \frac{\sigma_1^2}{2})(1 - \mathcal{R}_0^E) > 0$ . In particular, if  $\epsilon \leq P(0)$ , then for some sufficiently small  $\delta \in (0, 1)$ , one has

$$\mathbb{P}\{P(t) \leq \epsilon\} \geq 1 - \delta, \quad \forall t \geq \frac{(\sigma_1 \Phi_{1-\delta} + \sqrt{\sigma_1^2 \Phi_{1-\delta}^2 + 4\beta \ln \frac{P(0)}{\epsilon}})^2}{4\beta^2} \text{ a.s.}$$



**Proof** We consider the following auxiliary one-dimensional SDE:

$$dU(t) = \left( R_{\text{esp}} + \frac{\sigma_1^2}{2} \right) (\mathcal{R}_0^E - 1) dt + \sigma_1 dB_1(t) \tag{5.5}$$

with the initial value  $U(0) = \ln P(0)$ . Let  $U(t)$  be the solution of Eq. (5.5), by direct calculation, Eq. (5.5) has a unique explicit solution

$$U(t) = -\beta t + U(0) + \int_0^t \sigma_1 dB_1(\zeta).$$

Since  $B_1(t)$  is a standard Brownian motion, we obtain that  $B_1(0) = 0$  and  $B_1(t) \sim \mathbb{N}(0, t)$  for any  $t > 0$ , which means that  $\int_0^t \sigma_1 dB_1(\zeta) = B_1(t)$  and  $\frac{B_1(t)}{\sqrt{t}} \sim \mathbb{N}(0, 1)$ . Thus,

$$\begin{aligned} \mathbb{P}\{U(t) \leq \ln \epsilon\} &= \mathbb{P}\{-\beta t + U(0) + \sigma_1 B_1(t) \leq \ln \epsilon\} \\ &= \mathbb{P}\left\{ \frac{B_1(t)}{\sqrt{t}} \leq \frac{\beta t + \ln \epsilon - \ln P(0)}{\sigma_1 \sqrt{t}} \right\} \\ &= \Phi\left( \frac{\beta t + \ln \epsilon - \ln P(0)}{\sigma_1 \sqrt{t}} \right). \end{aligned} \tag{5.6}$$

Applying the comparison theorem of one-dimensional SDE (Ikeda and Watanade 1977), we then obtain from Eqs. (5.2) and (5.5) that  $\ln P(t) \leq U(t)$  for any  $t > 0$  a.s. Combining (5.6), one can see that

$$\mathbb{P}\{P(t) \leq \epsilon\} = \mathbb{P}\{\ln P(t) \leq \ln \epsilon\} \geq \Phi\left( \frac{\beta t + \ln \epsilon - \ln P(0)}{\sigma_1 \sqrt{t}} \right) \text{ a.s.} \tag{5.7}$$

In particular, if  $\epsilon \leq P(0)$ , we define  $\varphi(t) = \frac{\beta t + \ln \epsilon - \ln P(0)}{\sigma_1 \sqrt{t}}$  ( $t > 0$ ). It is clear to see that  $\varphi(t)$  and  $\Phi(\varphi(t))$  are both monotonically increasing functions on  $(0, \infty)$ . Note that  $\lim_{t \rightarrow \infty} \Phi(\varphi(t)) = \Phi(\infty) = 1$ . Combined with (5.7), we determine that for any small  $\delta \in (0, 1)$ , there exists a constant  $t_\epsilon^{(1-\delta)} = \frac{(\sigma_1 \Phi_{1-\delta} + \sqrt{\sigma_1^2 \Phi_{1-\delta}^2 + 4\beta \ln \frac{P(0)}{\epsilon}})^2}{4\beta^2}$  such that  $\varphi(t_\epsilon^{(1-\delta)}) = \Phi_{1-\delta}$  and

$$\mathbb{P}\{P(t) \leq \epsilon\} \geq \Phi(\varphi(t_\epsilon^{(1-\delta)})) = 1 - \delta, \quad \forall t \geq t_\epsilon^{(1-\delta)} \text{ a.s.} \tag{5.8}$$

Hence, this completes the proof of Theorem 5.2. □

**Remark 5.2** By (5.8),  $t_\epsilon^{(1-\delta)}$  is an increasing function with respect to  $P(0)$ , which implies that the initial value  $P(0)$  has a negative influence on the extinction of vegetation in system (1.2). In practice, the initial state of the vegetation in an arid ecosystem is not usually considered an extinction state. Thus, we need to choose the index  $\epsilon$  satisfying  $\epsilon \leq P(0)$ . Combining Theorem 5.2 and  $\Phi_{0.999} = 3.09$ , we can determine that the probability of vegetation extinction is at least 99.9% when

$t \geq t_{\epsilon}^{(0.999)} = \frac{(3.09\sigma_1 + \sqrt{9.5481\sigma_1^2 + 4\beta \ln \frac{P(0)}{\epsilon}})^2}{4\beta^2}$ . This implies that  $t_{\epsilon}^{(0.999)}$  can be regarded as the maximal extinction time of vegetation if the probability of error does not exceed 0.1%. In summary, we call  $t_{\epsilon}^{(1-\delta)}$  the maximum vegetation extinction time in the sense of at least probability  $1 - \delta$ .

### 6 Numerical Simulations

In this section, we will introduce Milstein’s higher-order method (Higham 2001) to verify our theoretical results. For any finite time interval  $[0, T_0]$ , the corresponding discretization equation of system (1.2) on  $t \in [0, T_0]$  is obtained as follows:

$$\begin{cases} P^{j+1} = P^j + \left( \frac{c\alpha_2 g_{CO_2} W^j P^j}{W^j + k_1} - R_{\text{esp}} P^j \right) \Delta t + \sigma_1 P^j \sqrt{\Delta t} \xi_j + \frac{\sigma_1^2 P^j}{2} (\xi_j^2 - 1) \Delta t \\ W^{j+1} = W^j + \left[ \frac{\alpha(P^j + k_2 w_0) S^j}{P^j + k_2} - \frac{q\alpha_2 \gamma g_{CO_2} W^j P^j}{W^j + k_1} - r_w W^j \right] \Delta t \\ \quad + \sigma_2 W^j \sqrt{\Delta t} \eta_j + \frac{\sigma_2^2 W^j}{2} (\eta_j^2 - 1) \Delta t, \\ S^{j+1} = S^j + \left[ R - \frac{\alpha(P^j + k_2 w_0) S^j}{P^j + k_2} \right] \Delta t + \sigma_3 S^j \sqrt{\Delta t} \zeta_j + \frac{\sigma_3^2 S^j}{2} (\zeta_j^2 - 1) \Delta t, \end{cases}$$

where  $\xi_j, \eta_j$  and  $\zeta_j$  ( $j = 1, 2, \dots, n$ ) are three independent random variables which follow the Gaussian distribution  $\mathbb{N}(0, 1)$ .  $n$  is the total number of iterations,  $\Delta t$  is the length of one iteration step. Moreover,  $(P^j, W^j, S^j)^T$  is the value of the  $j$ th iteration of the discretized equation. Based on some actual experimental data from Wuwei in China (from 2001 to 2019) (Chen et al. 2021), Yushu in China (from 1951 to 2008) (Yang et al. 2016) and Sahel (from 2002 to 2007) (Kefi et al. 2008), the corresponding average physiological parameters in system (1.2) are shown in Table 1.

Throughout the remainder of this section, we choose  $\Delta t = 0.001$  days. By a standard argument (Chen et al. 2021; Kefi et al. 2008, 2010), we obtain that  $R_{\text{esp}}$  and  $q$  are both monotonically increasing functions of the air temperature  $T_e$ . In addition,  $c$  is a monotonically increasing function with respect to the air CO<sub>2</sub> concentration ( $C_a$ ). They satisfy:

$$R_{\text{esp}} = R_b Q_{10}^{\frac{T_e - 10}{10}}, \quad q = 0.00482(1 - Rh)e^{\frac{17.502T_e}{T_e + 240.97}}, \quad c = m_0 C_a, \quad (6.1)$$

where  $R_b$  is the respiration per unit of vegetation biomass ( $\text{day}^{-1}$ ),  $Q_{10}$  is a Michaelis function and  $m_0$  is the coefficient of conversion of photosynthesis ( $\text{mol}$ ) into vegetation biomass ( $g$ ).  $Rh$  is the air relative humidity. According to Chen et al. (2021), Kefi et al. (2008), the values of these parameters are given by  $R_b = 0.1$ ,  $Q_{10} = 1.6$ ,  $Rh = 40\%$  and  $m_0 = 4.8$ . Using (6.1), the corresponding climatic parameters in Wuwei, Yushu and Sahel are obtained and shown in Table 2. To better study the mechanism of desertification formation, some future climatic scenarios in arid ecosystems should be introduced. Thus, Table 2 also presents two future climatic scenarios RCP4.5 and RCP8.5 of Wuwei.

**Table 2** List of values of the climatic parameters of system (1.2) under different regions and future climatic scenarios

Regions/climatic scenarios	$C_a$ (ppm)	$T_c$ (°C)	$R$ (mm day <sup>-1</sup> )	$R_{\text{esp}}$ (day <sup>-1</sup> )	$c$ (g mol <sup>-1</sup> )	$q$
Sahel	360	28.00	1.00	0.23303	1440	0.0179
Yushu	385	4.00	1.29	0.07543	1848	0.0038
Wuwei	400	8.00	0.85	0.09103	1920	0.0051
RCP4.5	542	8.65	0.73	0.09385	2601.6	0.0053
RCP8.5	563	13.00	0.68	0.11514	2702.4	0.0071

By means of different combinations of stochastic noise and climatic parameters, we will numerically focus on the following four aspects:

- (i) The equilibria and related stability of deterministic system (1.1).
- (ii) The impact of stochastic noise and rainfall rate on vegetation dynamics of system (1.2).
- (iii) The existence of the ergodic stationary distribution  $\varpi(\cdot)$  of system (1.2) under  $\mathcal{R}_0^H > 1$ , and the explicit expression and the local fitting effect of the approximate probability density function of the stationary distribution  $\varpi(\cdot)$ .
- (iv) Vegetation extinction and the expected extinction time of system (1.2) under  $\mathcal{R}_0^E < 1$ .

**Remark 6.1** As is well known, the unique stationary distribution  $\varpi(\cdot)$  under  $\mathcal{R}_0^H > 1$  denotes a long-time, stochastic, positive steady state of the vegetation of system (1.2) and is a distribution function defined in infinite time. The existence of the distribution  $\varpi(\cdot)$  cannot be directly verified due to the finite number of iterations of the computer simulation. According to Zhou et al. (2021), for any finite time interval  $[0, T_0]$ , if  $\mathcal{R}_0^H > 1$ , system (1.2) will have a transient distribution function  $\tilde{\varpi}(\cdot, T_0)$  that relies on the variable  $T_0$ , and the function  $\tilde{\varpi}(\cdot, T_0)$  can reflect most of the dynamic behavior of  $\varpi(\cdot)$ . In addition, for some sufficiently large  $T_0$ ,  $\tilde{\varpi}(\cdot, T_0)$  will fluctuate around  $\varpi(\cdot)$  and satisfies  $\lim_{T_0 \rightarrow \infty} \tilde{\varpi}(\cdot, T_0) = \varpi(\cdot)$  Zhou et al. (2021). Hence, we will use the transient distribution function  $\tilde{\varpi}(\cdot, T_0)$  with a large enough time interval and a sufficient number of iterations to indirectly examine the existence of the distribution  $\varpi(\cdot)$  of system (1.2) under  $\mathcal{R}_0^H > 1$ .

## 6.1 Equilibria and Related Stability of Deterministic System (1.1)

In this section, we select the initial value of deterministic system (1.1) and the total time of iterations as  $(P(0), W(0), S(0))^T = (500, 40, 5)^T$  and  $T_0 = 400$  days, respectively. Next, we will use system (1.1) to describe the vegetation dynamics of Wuwei, Yushu and Sahel.

**Example 6.1** According to the relevant climatic parameters of Sahel in Table 2, we compute that  $\mathcal{R}_0 = 0.8033$ . By Theorem A.1, system (1.1) has an LAS vegetation-free equilibrium  $D_0$ , which implies that the vegetation  $P$  in Sahel will go to extinction (i.e.,  $P(t) \rightarrow 0$  as  $t \rightarrow \infty$ ) without human intervention. Figure 2a–c can illustrate it. Using the climatic parameters of Wuwei in Table 2, a direct calculation shows that  $\mathcal{R}_0 = 3.5883$  and  $\mathcal{R}_1 = 7.5494 \times 10^{16}$ . According to Theorem A.2, system (1.1) has an LAS vegetation-positive equilibrium  $D^*$ . This means that the vegetation in Yushu will be persistent, which is supported in Fig. 2d–f. For the climatic parameters of Wuwei, we have  $\mathcal{R}_0 = 2.5196$  and  $\mathcal{R}_1 = 1.0023 \times 10^{16}$ . Figure 2g–i shows that the vegetation in Wuwei will have a stable positive equilibrium state, which is consistent with Theorem A.2.

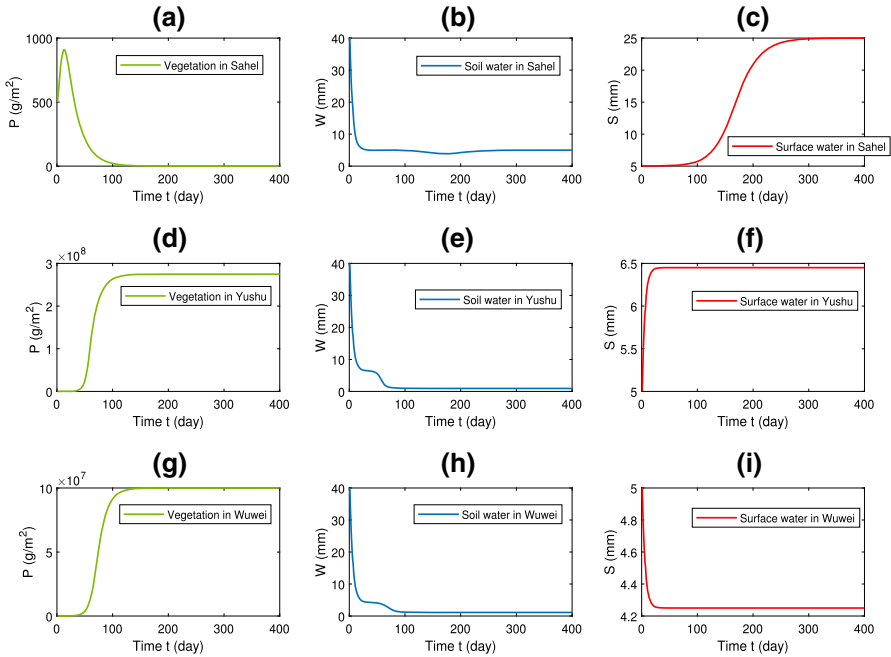


**Fig. 2** a–c The solution of system (1.1) with the climatic parameters of Sahel; d–f the solution of system (1.1) with the climatic parameters of Yushu; g–i: the solution of system (1.1) with the climatic parameters of Wuwei. All the observation interval are  $[0, 400]$  (day), and the number of observations in the interval  $[0, 400]$  is 400,000

### 6.2 Impact of Rainfall Rate $R$

It is well known that semi-arid area refers to climate type area with average annual precipitation between 200 and 500 mm (i.e.,  $0.5479 \leq R \leq 1.3699$ ). Similar to Sect 6.1, we will use stochastic system (1.2) to describe the vegetation dynamics of Sahel. Moreover, let  $(P(0), W(0), S(0))^T = (500, 40, 5)^T$  be the initial value of system (1.2).

**Example 6.2** We fix  $T_0 = 1600$  days and consider three cases of the noise intensity:

- (i)  $(\sigma_1, \sigma_2, \sigma_3) = (0.01, 0.01, 0.01)$ ,   (ii)  $(\sigma_1, \sigma_2, \sigma_3) = (0.04, 0.04, 0.04)$ ,
- (iii)  $(\sigma_1, \sigma_2, \sigma_3) = (0.1, 0.1, 0.1)$ .

Using the variable-controlling approach, we will fix the values of the  $\text{CO}_2$  concentration and air temperature in Sahel. That is,  $R_{\text{esp}} \equiv 0.23303$ ,  $c \equiv 1440$  and  $q \equiv 0.0179$ . Figure 3 presents the variation trends of  $\mathcal{P}_0^H$  with different  $R \in [0.4, 3]$ . According to Theorem 3.1, we can determine that the rainfall rate is helpful for the persistence of vegetation in Sahel for all cases (i)–(iii). In particular, under case (i), we can take some effective measures such as artificial rainfall, to make  $R \geq 1.656$  ( $\text{mm day}^{-1}$ ) to maintain vegetation persistence in Sahel. Moreover, we consider the following four

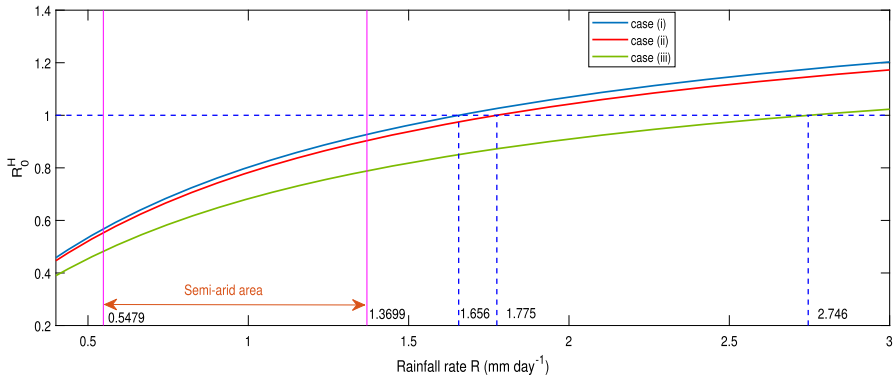


**Fig. 3** The variation trends of  $\mathcal{R}_0^H$  with different rainfall rates  $R \in [0.4, 3]$  and different cases of noise intensity, where case (i):  $(\sigma_1, \sigma_2, \sigma_3) = (0.01, 0.01, 0.01)$ , case (ii):  $(\sigma_1, \sigma_2, \sigma_3) = (0.04, 0.04, 0.04)$  and case (iii):  $(\sigma_1, \sigma_2, \sigma_3) = (0.1, 0.1, 0.1)$ . Other fixed parameters:  $(R_{\text{esp}}, c, q) = (0.23303, 1440, 0.0179)$

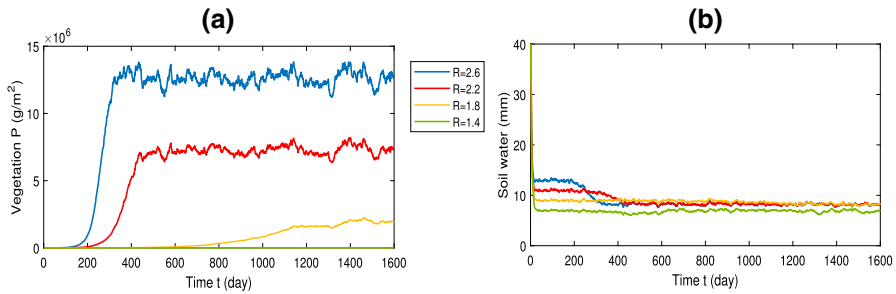


**Fig. 4** The diagram tracks variation trends of vegetation  $P(t)$  and soil water  $W(t)$  of system (1.2) with different rainfall rates  $R = 2.6, 2.2, 1.8$  and  $1.4$ . Other parameters are the same as in Fig. 3. The observation interval is  $[0, 1600]$  (day), and the number of observations in the interval  $[0, 1600]$  is 1,600,000

cases of  $R$  under case (i):

$$(\mathcal{E}_1) R = 2.6, \quad (\mathcal{E}_2) R = 2.2, \quad (\mathcal{E}_3) R = 1.8, \quad (\mathcal{E}_4) R = 1.4.$$

Figure 4 shows the corresponding variation trends of the vegetation  $P(t)$  and soil water  $W(t)$  of system (1.2) under case (i). Clearly, we obtain from Fig. 4a that the vegetation of system (1.2) will shift from a dense state to a sparse state or even desertification as the value of  $R$  decreases.

Based on the expression of  $\mathcal{R}_0^H$ , Figs. 3 and 4, we conclude that the rainfall rate has a positive influence on prompting the persistence of vegetation. Furthermore, the critical value  $R$  satisfying  $\mathcal{R}_0^H > 1$  will increase as the noise intensity increases. This implies that the impact of the holistic noise intensity  $(\sigma_1, \sigma_2, \sigma_3)$  on vegetation persistence is negative.

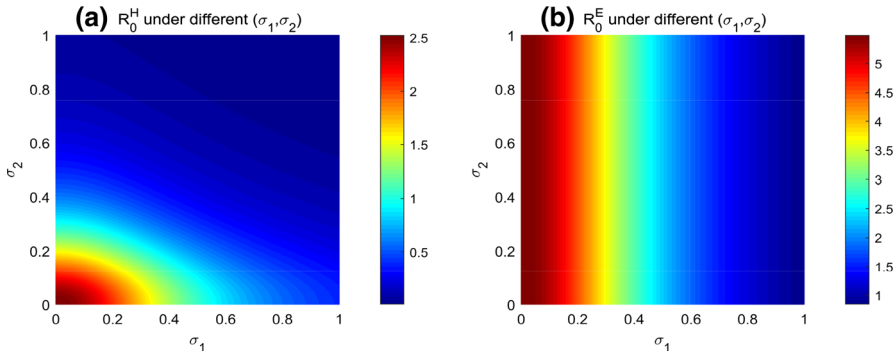


**Fig. 5** The color phase diagrams for the variation trends of  $\mathcal{R}_0^H$  and  $\mathcal{R}_0^E$  with different noise intensities  $(\sigma_1, \sigma_2) \subseteq [0, 1] \times [0, 1]$  (Color figure online)

### 6.3 Impact of Noise Intensities $\sigma_i$ ( $i = 1, 2, 3$ )

According to Sect. 6.2, we will separately study the impacts of  $\sigma_1, \sigma_2$  and  $\sigma_3$  on vegetation dynamics. Note that the values of  $\mathcal{R}_0^H$  and  $\mathcal{R}_0^E$  are both affected by the noise intensity  $\sigma_1$ ; thus, the impact of  $\sigma_1$  should be emphatically analyzed.

#### 6.3.1 Impact of $\sigma_1$

In this subsection, we will study the dynamical behavior of system (1.2) based on the climatic data from Wuwei. For simplicity, we assume that  $\sigma_2 = \sigma_3$ . Figure 5 shows the color phase diagrams for the variation trends of  $\mathcal{R}_0^H$  and  $\mathcal{R}_0^E$  with different stochastic noises  $(\sigma_1, \sigma_2) \subseteq [0, 1] \times [0, 1]$ . Combined with Theorems 3.1 and 5.1, for any initial value  $(P(0), W(0), S(0))^T \in \mathbb{R}_+^3$ , the vegetation will be coexistent with the water environment in the long term if  $(\sigma_1, \sigma_2) \subseteq [0, 0.2] \times [0, 0.2]$ , but it will go to extinction when  $\sigma_1 \geq 0.92$ .

**Example 6.3** We select the initial value  $(P(0), W(0), S(0))^T = (1250, 2, 3)^T$  and  $\sigma_2 = 0.001$ . As shown in Fig. 5, we consider the following five cases of  $\sigma_1$ :

- (i)  $\sigma_1 = 0.01$ , (ii)  $\sigma_1 = 0.1$ , (iii)  $\sigma_1 = 0.6$ , (iv)  $\sigma_1 = 0.8$ , (v)  $\sigma_1 = 1$ .

For case (i), a direct calculation shows that  $\mathcal{R}_0^H = 2.5182$ . On the one hand, according to Theorem 3.1, the solution  $Q(t)$  of system (1.2) has a unique stationary distribution  $\varpi(\cdot)$ . Based on Remark 6.1, we select the observation interval as  $[0, 50,000]$  (day), i.e.,  $T_0 = 50,000$  days. The corresponding marginal frequency histograms of  $P, W$  and  $S$  with respect to the transient distribution  $\tilde{\varpi}(\cdot, 50,000)$  are shown in the right-hand column of Fig. 6. This indirectly verifies the existence of the distribution  $\varpi(\cdot)$ . Furthermore, the left-hand column of Fig. 6 presents the corresponding solutions of systems (1.1) and (1.2) within 5000 days. On the other hand, we compute that  $\mathcal{R}_1^C = 5.2596 \times 10^{-6}$ ,  $\bar{D}^* = (100036023.45, 1.1158, 4.2500)^T$ ,  $\lambda_3 = 0.0084$  and  $\lambda_1\lambda_2 - \lambda_3 = 0.1409$ . By Theorem 4.1, the distribution  $\varpi(\cdot)$  around  $\bar{D}^*$  approximately

has a three-dimensional log-normal density function  $\Upsilon(P, W, S)$ . Combined with  $\Delta = -3.2260 \times 10^7$ , we obtain that

$$\Sigma = \begin{pmatrix} 0.0008652 & -0.0006715 & 0.0000007 \\ -0.0006715 & 0.000575 & 0.0000018 \\ 0.0000007 & 0.0000018 & 0.0000025 \end{pmatrix}.$$

Then, it follows from Remark r4.1 that  $\Upsilon(P, W, S)$  has the following three marginal density functions:

$$\begin{aligned} \ell_1(P) &= \frac{13.563}{P} e^{-577.901(\ln \frac{P}{100036023.45})^2}, \quad \ell_2(W) = \frac{16.637}{W} e^{-869.565(\ln \frac{W}{1.1158})^2}, \\ \ell_3(S) &= \frac{252.313}{S} e^{-200000(\ln \frac{S}{4.25})^2}. \end{aligned}$$

To verify the correctness of Theorem 4.1 and study the local fitting effect of  $\Upsilon(P, W, S)$ , based on the command “ksdensity(·, ·)” in MATLAB (MathWorks, R2019b), we plot the frequency histogram fitting curves of  $P, W$  and  $S$  at the iteration time equals to 10,000, 20,000 and 40,000 days, each in a different color. Clearly, the above functions  $\ell_1(P), \ell_2(W)$  and  $\ell_3(S)$  all almost coincide with the corresponding three fitting curves, see Fig. 7. To conceptualize this more intuitively, we assume the three fitting curves of  $(P, W, S)$  as  $(\tilde{h}_1(P, j), \tilde{h}_2(W, j), \tilde{h}_3(S, j))$  ( $j = 10,000, 20,000, 40,000$ ). In the observation interval of the value of  $(P, W, S)$  in Fig. 7, by selecting 5000 equidistant observation points, we further define  $e_a^{(m)}(P, i), \bar{e}_a(P, i)$  and  $\bar{e}_r(P, i)$  as the maximum and average absolute errors, and the average relative error between the functions  $\ell_1(P)$  and  $\tilde{h}_1(P, i)$ , respectively,  $i = 10,000, 20,000, 40,000$ . The relevant notations for the variables  $W$  and  $S$  can be similarly defined. Table 3 shows the corresponding error values of  $(P, W, S)$  at different iteration times. Evidently, all the average relative errors inspected are less than 5%. This together with Fig. 7 means that the fitting effect of  $\ell_1(P), \ell_2(W)$  and  $\ell_3(S)$  for the corresponding theoretical marginal densities of the distribution  $\varpi(\cdot)$  is not only local but also global. That is to say, the global density function of the distribution  $\varpi(\cdot)$  can be greatly approximated by  $\Upsilon(P, W, S)$ . Thus, Theorem 4.1 and  $\Upsilon(P, W, S)$  are well verified. Additionally, we plot the functions  $\ell_1(P), \ell_2(W)$  and  $\ell_3(S)$  in the right-hand column of Fig. 6. They also have a good approximation for the marginal frequency histograms of the transient distribution  $\tilde{\varpi}(\cdot, 50,000)$ .

For case (ii), we obtain that  $\mathcal{R}_0^H = 2.3884, \bar{D}^* = (92606371.95, 1.1909, 4.2501)^T, \mathcal{R}_1^C = 5.5721 \times 10^{-6}, \lambda_3 = 0.008$  and  $\lambda_1 \lambda_2 - \lambda_3 = 0.1247$ . Thus, by Theorems 3.1 and 4.1, the solution  $Q(t)$  of system (1.2) still has a unique stationary distribution  $\varpi(\cdot)$ , and  $\varpi(\cdot)$  around the equilibrium  $\bar{D}^*$  approximately has a log-normal density function  $\Upsilon(P, W, S)$ . In this example, we still select  $T_0 = 50,000$  days. Then by calculation, we have  $\Delta = -2.4673 \times 10^7 \neq 0$ , and the marginal densities of the function  $\Upsilon(P, W, S)$  are obtained by  $\ell_1(P) = \frac{1.366}{P} e^{-5.8617(\ln \frac{P}{92606371.95})^2}, \ell_2(W) = \frac{1.7184}{W} e^{-9.2764(\ln \frac{W}{1.1909})^2}$  and  $\ell_3(S) = \frac{252.313}{S} e^{-200000(\ln \frac{S}{4.2501})^2}$ .



**Table 3** List of the errors ( $e_a^{(m)}(P, \cdot), e_a^{(m)}(W, \cdot), e_a^{(m)}(S, \cdot), (\bar{e}_a(P, \cdot), \bar{e}_a(W, \cdot), \bar{e}_a(S, \cdot))$  and  $(\bar{e}_r(P, \cdot), \bar{e}_r(W, \cdot), \bar{e}_r(S, \cdot))$  in the observation interval  $[8 \times 10^7, 1.2 \times 10^8] \times [0.8, 1.4] \times [4.2, 4.3]$  at different iteration times ( $\sigma_1 = 0.01, \sigma_2 = \sigma_3 = 0.001$ )

Time interval $[0, T_0]$ (day)	[0, 10,000]	[0, 20,000]	[0, 40,000]
$(e_a^{(m)}(P, \cdot), e_a^{(m)}(W, \cdot), e_a^{(m)}(S, \cdot))$	$(5.219 \times 10^{-9}, 0.799, 0.702)$	$(3.735 \times 10^{-9}, 0.317, 1.594)$	$(9.176 \times 10^{-9}, 1.177, 0.996)$
$(\bar{e}_a(P, \cdot), \bar{e}_a(W, \cdot), \bar{e}_a(S, \cdot))$	$(9.830 \times 10^{-10}, 0.267, 0.161)$	$(9.401 \times 10^{-10}, 0.155, 0.522)$	$(2.334 \times 10^{-9}, 0.537, 0.387)$
$(\bar{e}_r(P, \cdot), \bar{e}_r(W, \cdot), \bar{e}_r(S, \cdot))$	$(2.13\%, 1.63\%, 0.28\%)$	$(1.41\%, 1.46\%, 0.52\%)$	$(4.09\%, 4.29\%, 0.87\%)$

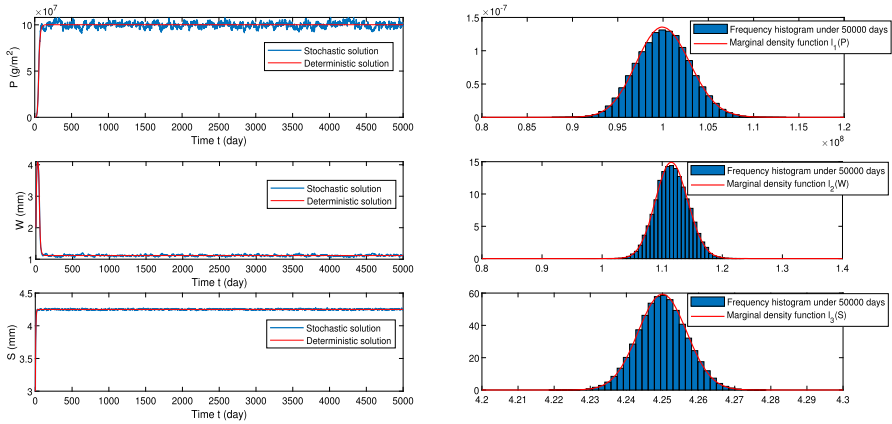


**Fig. 6** The left-hand column shows the solutions of deterministic system (1.1) and of stochastic system (1.2) on  $t \in [0, 5000]$  (day). The right-hand column presents the frequency histograms with 50,000,000 iteration points (i.e.,  $T_0 = 50,000$  days), and the marginal densities  $\ell_1(P)$ ,  $\ell_2(W)$  and  $\ell_3(S)$  of the approximate density function  $\mathfrak{T}(P, W, S)$ . Fixed parameters:  $(P(0), W(0), S(0))^T = (1250, 2, 3)^T$ ,  $\sigma_1 = 0.01$ ,  $\sigma_2 = \sigma_3 = 0.001$

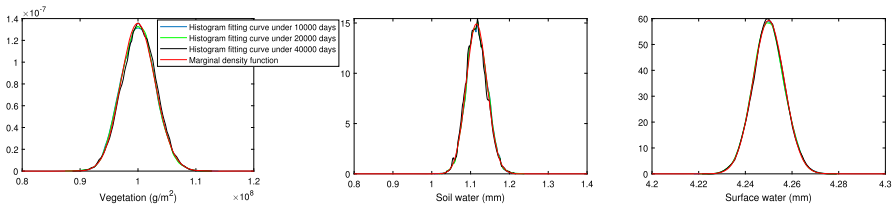


**Fig. 7** The blue, green and black lines separately represent the frequency histogram fitting curves of the subpopulations  $P$ ,  $W$  and  $S$  with the iteration time equals to 10,000, 20,000 and 40,000 days of the total time  $T_0$ . The red lines denote the corresponding marginal densities  $\ell_1(P)$ ,  $\ell_2(W)$  and  $\ell_3(S)$  of the approximate density function  $\mathfrak{T}(P, W, S)$ . All of the parameter values are the same as in Fig. 6 (Color figure online)

Analogous to case (i), we first plot the frequency histograms of  $P$ ,  $W$  and  $S$  with respect to the transient distribution  $\tilde{\varpi}(\cdot, 50,000)$ , see the right-hand column of Fig. 8. Evidently, the existence of the distribution  $\varpi(\cdot)$  are indirectly verified. Compared with the above functions  $\ell_1(P)$ ,  $\ell_2(W)$  and  $\ell_3(S)$ , Fig. 9 presents the frequency histogram fitting curves of the subpopulations  $P$ ,  $W$  and  $S$  at the iteration time equals to 10,000, 20,000 and 40,000 days of the total time  $T_0$ , each in a different color. Moreover, we still select 5000 equidistant observation points in the observation interval of the value of  $(P, W, S)$  in Fig. 9, and the corresponding errors  $e_a^{(m)}(\cdot, \cdot)$ ,  $\bar{e}_a(\cdot, \cdot)$  and  $\bar{e}_r(\cdot, \cdot)$  of  $(P, W, S)$  at different iteration times are presented in Table 4. It can be easily noticed from Fig. 9 and Table 4 that the functions  $\ell_1(P)$ ,  $\ell_2(W)$  and  $\ell_3(S)$  all almost coincide with the corresponding three fitting curves. Thus, the local approximate density function  $\mathfrak{T}(P, W, S)$  has a good global fitting effect for the theoretical density function of the distribution  $\varpi(\cdot)$ . These verify  $\mathfrak{T}(P, W, S)$  and Theorem 4.1 again.

**Table 4** List of the errors ( $e_a^{(m)}(P, \cdot), e_a^{(m)}(W, \cdot), e_a^{(m)}(S, \cdot), \bar{e}_a(P, \cdot), \bar{e}_a(W, \cdot), \bar{e}_a(S, \cdot)$ ) and ( $\bar{e}_r(P, \cdot), \bar{e}_r(W, \cdot), \bar{e}_r(S, \cdot)$ ) in the observation interval  $[0, 1.2 \times 10^8] \times [0.2, 3] \times [4.2, 4.3]$  at different iteration times ( $\sigma_1 = 0.1, \sigma_2 = \sigma_3 = 0.001$ )

Time interval $[0, T_0]$ (day)	$[0, 10,000]$	$[0, 20,000]$	$[0, 40,000]$
$(e_a^{(m)}(P, \cdot), e_a^{(m)}(W, \cdot), e_a^{(m)}(S, \cdot))$	$(4.168 \times 10^{-9}, 0.095, 1.497)$	$(4.601 \times 10^{-9}, 0.089, 1.879)$	$(7.441 \times 10^{-9}, 0.109, 2.137)$
$(\bar{e}_a(P, \cdot), \bar{e}_a(W, \cdot), \bar{e}_a(S, \cdot))$	$(9.251 \times 10^{-10}, 0.049, 0.452)$	$(9.224 \times 10^{-10}, 0.046, 0.493)$	$(1.886 \times 10^{-9}, 0.074, 0.529)$
$(\bar{e}_r(P, \cdot), \bar{e}_r(W, \cdot), \bar{e}_r(S, \cdot))$	$(1.92\%, 3.94\%, 0.43\%)$	$(2.03\%, 3.82\%, 0.48\%)$	$(3.92\%, 6.07\%, 0.94\%)$

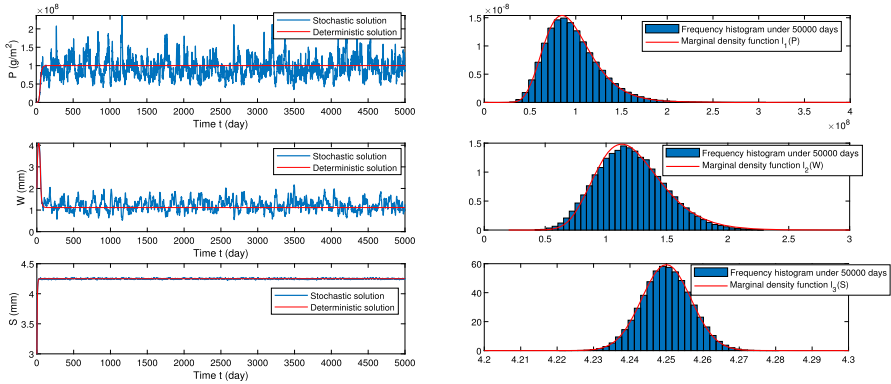


**Fig. 8** The left-hand column shows the solutions of deterministic system (1.1) and of stochastic system (1.2) on  $t \in [0, 5000]$  (day). The right-hand column presents the frequency histograms with the iteration time  $T_0 = 50,000$  days, and the marginal densities  $\ell_1(P)$ ,  $\ell_2(W)$  and  $\ell_3(S)$  of the approximate density function  $\Upsilon(P, W, S)$ . A fixed parameter:  $\sigma_1 = 0.1$ . The other fixed parameter values and the observation interval are the same as Fig. 6

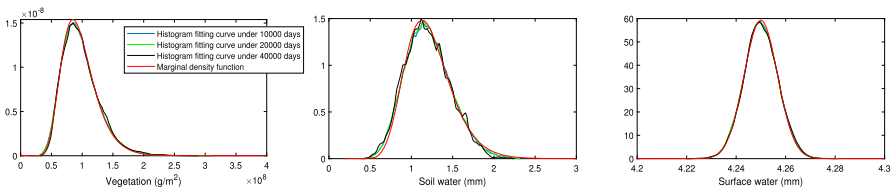


**Fig. 9** The blue, green and black lines separately denote the frequency histogram fitting curves of the subpopulations  $P$ ,  $W$  and  $S$  with the iteration time equals to 10,000, 20,000 and 40,000 days of the total time  $T_0$ . The red lines represent the marginal densities  $\ell_1(P)$ ,  $\ell_2(W)$  and  $\ell_3(S)$  of the approximate density function  $\Upsilon(P, W, S)$ . All of the parameter values are the same as in Fig. 8

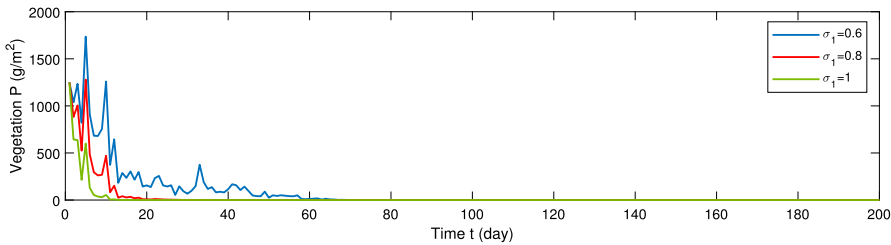


**Fig. 10** Computer simulations for variation trends of vegetation  $P(t)$  of system (1.2) with different noise intensities  $\sigma_1 = 0.6, 0.8$  and 1. The observation interval is  $[0, 200]$  (day), and the number of observations in the interval  $[0, 200]$  is 200,000. The other fixed parameter values and the observation interval are the same as Fig. 6

For cases (iii)–(v), Fig. 10 presents the corresponding variation trends of the vegetation  $P(t)$  of system (1.2). It is clear that the vegetation of system (1.2) will go to extinction for all cases (iii)–(v). Moreover, as the noise intensity  $\sigma_1$  increases, the extinction time decreases. In particular, we compute  $\mathcal{R}_0^H = 0.3881$  and  $\mathcal{R}_0^E = 0.8446$  under case (v). Combined with the green line in Fig. 10, Theorem 5.1 is well verified.

**Table 5** List of values of  $\mathcal{R}_0^E, t_\epsilon^{(0.90)}$  and  $t_\epsilon^{(0.99)}$  under different cases (i)–(viii) of the parameters  $(P(0), \sigma_1)$

$(P(0), \sigma_1)$	(i)	(ii)	(iii)	(iv)	(v)	(vi)	(vii)	(viii)
$t_\epsilon^{(0.90)}$ (day)	328.27	315.91	299.33	286.57	100.36	95.11	88.05	82.61
$t_\epsilon^{(0.99)}$ (day)	785.28	771.45	753.01	738.92	203.8a5	197.81	189.72	183.51
$\mathcal{R}_0^E$	0.8446	0.8446	0.8446	0.8446	0.7172	0.7172	0.7172	0.7172

In summary, we obtain that the impact of noise intensity  $\sigma_1$  on vegetation stability of system (1.2) is generally negative. Specifically, based on cases (i)–(ii), Figs. 7 and 9, it has numerically shown that for some small  $\sigma_1$ , the vegetation  $P(t)$  will be persistent and the solution  $Q(t)$  of system (1.2) has a unique stationary distribution. As the value of  $\sigma_1$  increases, the marginal distribution of the vegetation  $P(t)$  will become more scattered (see the right-hand columns of Figs. 6, 8), and even the vegetation will die out exponentially for some large  $\sigma_1$  (see Fig. 10). Below we will further study the impacts of the initial value  $P(0)$  and noise intensity  $\sigma_1$  on the extinction time of vegetation when  $\mathcal{R}_0^E < 1$ .

**Example 6.4** We fix  $(W(0), S(0), \sigma_2, \sigma_3) = (40, 5, 0.01, 0.01)$  and consider the following eight cases of the parameters  $(P(0), \sigma_1)$ , which include: (i) (10,000, 1), (ii) (5000, 1), (iii) (2000, 1), (iv) (1000, 1), (v) (10,000, 1.1), (vi) (5000, 1.1), (vii) (2000, 1.1) and (viii) (1000, 1.1).

According to Theorem 5.2, we choose the index of vegetation extinction as  $\epsilon = 10$  ( $g/m^2$ ). Combined with the expression of the maximum extinction time  $t_\epsilon^{(1-\delta)}$  of vegetation in (5.8), Table 5 presents the corresponding values of  $\mathcal{R}_0^E, t_\epsilon^{(0.90)}$  and  $t_\epsilon^{(0.99)}$  under different cases (i)–(viii).

For cases (i)–(iv), Fig. 11 presents the corresponding variation trends of vegetation  $P(t)$  of system (1.2) with the iteration time  $T_0 = 800$  days. Similarly, for cases (v)–(viii), the corresponding variation trends of vegetation  $P(t)$  with the iteration time  $T_0 = 300$  days are shown in Fig. 12. Combining Table 5, Figs. 11 and 12, we determine that the impacts of initial value  $P(0)$  and noise intensity  $\sigma_1$  have negative and positive effects on the extinction time of vegetation, respectively. That is to say, the vegetation  $P(t)$  of system (1.2) will die out faster as  $P(0)$  decreases or  $\sigma_1$  increases. Furthermore, it is clear that the vegetation  $P(t)$  will go to extinction when  $t \geq t_\epsilon^{(0.99)}$  for all cases (i)–(viii). This means that  $t_\epsilon^{(0.99)}$  can be used as a vegetation extinction time index applied in practice for some large  $\sigma_1$ . In this sense, Theorem 5.2 is well verified.

### 6.3.2 Impact of $\sigma_2$ and $\sigma_3$

In this subsection, we will analyze the vegetation dynamics of system (1.2) based on the climatic data from Yushu.

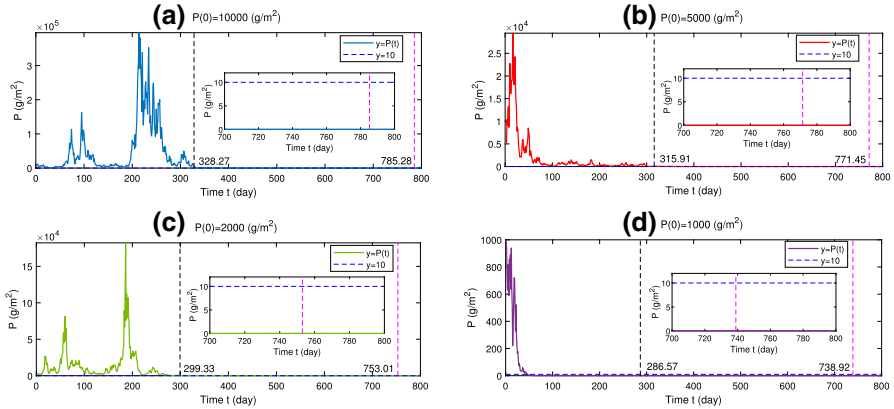


**Fig. 11** The solid blue, red, green and purple lines separately represent the variation trends of vegetation  $P(t)$  of system (1.2) with the initial values  $P(0) = 10,000, 5000, 2000$  and  $1000 \text{ (g/m}^2\text{)}$ . The dotted blue line is the measure of vegetation extinction. The dotted black and pink lines denotes the maximum extinction time of vegetation in the sense of at least probabilities 90% and 99%, respectively. Fixed parameters:  $(W(0), S(0), \sigma_1, \sigma_2, \sigma_3) = (40, 5, 1, 0.01, 0.01)$ . All the observation interval is  $[0, 800]$  (day), and the number of observations in the interval  $[0, 800]$  is 800,000 (Color figure online)

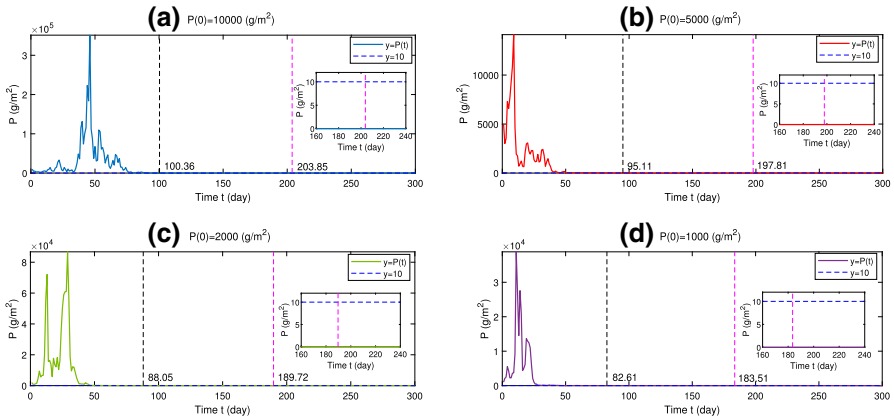


**Fig. 12** The solid blue, red, green and purple lines separately represent the variation trends of vegetation  $P(t)$  of system (1.2) with the initial values  $P(0) = 10,000, 5000, 2000$  and  $1000 \text{ (g/m}^2\text{)}$ . The dotted blue line is the measure of vegetation extinction. The dotted black and pink lines denote the maximum extinction time of vegetation in the sense of at least probabilities 90% and 99%, respectively. A fixed parameter:  $\sigma_1 = 1.1$ . The other fixed parameter values are the same as Fig. 11. All the observation interval is  $[0, 300]$  (day), and the number of observations in the interval  $[0, 300]$  is 300,000 (Color figure online)

**Example 6.5** Using the variable-controlling approach, we fix  $Q(0) = (200, 20, 5)^T$  and  $T_0 = 400$  days and consider the following seven cases of  $(\sigma_2, \sigma_3)$ :

- (i)  $(\sigma_2, \sigma_3) = (0.001, 0.001)$ , (ii)  $(\sigma_2, \sigma_3) = (0.05, 0.001)$ ,
- (iii)  $(\sigma_2, \sigma_3) = (0.2, 0.001)$ , (iv)  $(\sigma_2, \sigma_3) = (0.35, 0.001)$ ,
- (v)  $(\sigma_2, \sigma_3) = (0.001, 0.05)$ , (vi)  $(\sigma_2, \sigma_3) = (0.001, 0.2)$ ,

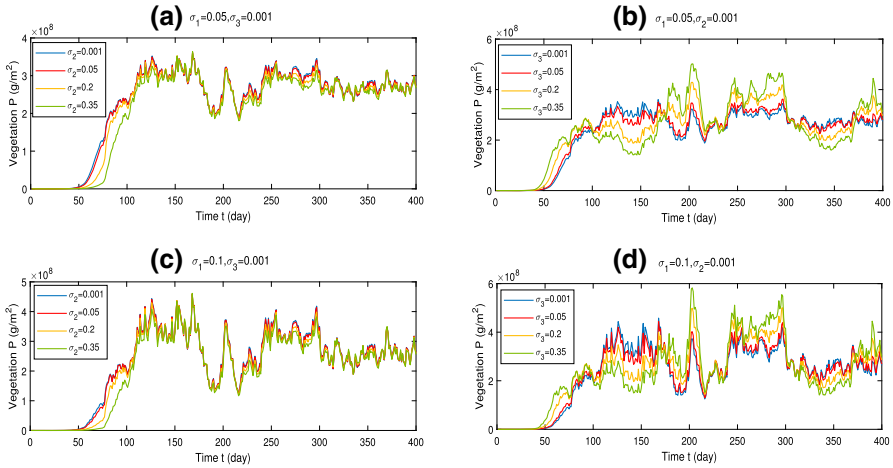


**Fig. 13** The diagram (a): Computer simulations for variation trends of vegetation  $P(t)$  of system (1.2) with different  $\sigma_2 = 0.001, 0.05, 0.2$  and  $0.35$  under  $(\sigma_1, \sigma_3) = (0.05, 0.001)$ ; The diagram (b): Computer simulations for variation trends of vegetation  $P(t)$  of system (1.2) with different  $\sigma_3 = 0.001, 0.05, 0.2$  and  $0.35$  under  $(\sigma_1, \sigma_2) = (0.05, 0.001)$ ; The diagram (c): Computer simulations for variation trends of vegetation  $P(t)$  of system (1.2) with different  $\sigma_2 = 0.001, 0.05, 0.2$  and  $0.35$  under  $(\sigma_1, \sigma_3) = (0.1, 0.001)$ ; The diagram (d): Computer simulations for variation trends of vegetation  $P(t)$  of system (1.2) with different  $\sigma_3 = 0.001, 0.05, 0.2$  and  $0.35$  under  $(\sigma_1, \sigma_2) = (0.1, 0.001)$ . Fixed parameters:  $Q(0) = (200, 20, 5)^T$ . All the observation interval are  $[0, 400]$  (day)

(vii)  $(\sigma_2, \sigma_3) = (0.001, 0.35)$ .

Moreover, we select two special values of  $\sigma_1$ , which includes: (I)  $\sigma_1 = 0.05$  and (II)  $\sigma_1 = 0.1$ . Figure 13 shows the corresponding variation trends of vegetation  $P(t)$  of system (1.2) under different cases (i)–(vii). Note that  $\mathcal{R}_0^H$  will decrease as the noise intensity  $\sigma_i$  increases,  $i = 1, 2, 3$ . Combined with  $\mathcal{R}_0^H = 1.0178$  when  $(\sigma_1, \sigma_2, \sigma_3) = (0.1, 0.35, 0.35)$ , we obtain that the vegetation  $P(t)$  of system (1.2) will be persistent for all cases (i)–(vii), which is supported in Fig. 13. On the one hand, it follows from Fig. 13a, c that the vegetation biomass will decrease slightly as the noise intensity  $\sigma_2$  increases. This implies that  $\sigma_2$  has a minor negative effect on vegetation growth. On the other hand, it can be noticed from Fig. 13b, d that the larger noise intensity  $\sigma_3$  is, the larger fluctuation (i.e., the larger variance) of the vegetation  $P(t)$  of system (1.2) is. Thus, the increase of noise intensity  $\sigma_3$  decreases the stability of stochastic positive equilibrium state of the vegetation of system (1.2).

### 6.4 Dynamical Analysis of Vegetation Under Future Climatic Scenarios

To better get a view of the trend of vegetation evolution, in this section, the dynamical behavior of vegetation  $P(t)$  of system (1.2) is investigated based on two future climatic scenarios RCP4.5 and RCP8.5 of Wuwei.

**Example 6.6** We select  $(P(0), W(0), S(0))^T = (1250, 20, 3)^T$ ,  $(\sigma_1, \sigma_2, \sigma_3) = (0.05, 0.001, 0.001)$  and  $T_0 = 50,000$  days. A direct calculation shows that  $\mathcal{R}_0^H =$

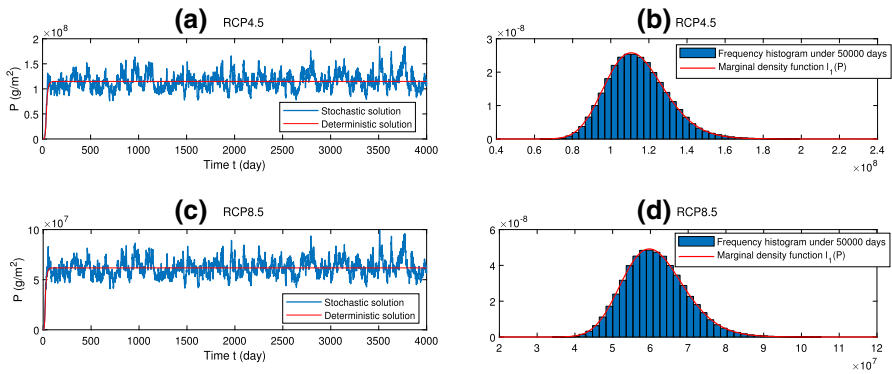


**Fig. 14** Figure 14a shows simulation of vegetation  $P(t)$  in deterministic system (1.1) and stochastic system (1.2) on  $t \in [0, 4000]$  (day) and under the scenario RCP4.5; Fig. 14b presents the frequency histogram with the iteration time  $T_0 = 50,000$  days, and the approximate density function  $\ell_1(P)$  of vegetation under the scenario RCP4.5; Fig. 14c shows simulation of vegetation  $P(t)$  in deterministic system (1.1) and stochastic system (1.2) on  $t \in [0, 4000]$  (day) and under the scenario RCP8.5; Fig. 14d presents the frequency histogram with the iteration time  $T_0 = 50,000$  days, and the approximate density function  $\ell_1(P)$  of vegetation under the scenario RCP8.5. Fixed parameters:  $(\sigma_1, \sigma_2, \sigma_3) = (0.05, 0.001, 0.001)$  and  $Q(0) = (1250, 2, 3)^T$

3.0013 and  $\ell_1(P) = \frac{2.8866}{P} e^{-26.178(\ln P - 18.5418)^2}$  under the scenario RCP4.5, and  $\mathcal{R}_0^H = 2.4434$  and  $\ell_1(P) = \frac{2.9653}{P} e^{-27.624(\ln P - 17.9229)^2}$  under the scenario RCP8.5. According to Remark 4.1 and Theorems 3.1, the vegetation  $P(t)$  of system (1.2) will be persistent and has a unique stationary marginal distribution  $\mu_1(P)$  under both the scenarios RCP4.5 and RCP8.5. Then, by Theorem 4.1, the corresponding density function of the distribution  $\mu_1(P)$  around  $\bar{P}^*$  can be approximated by  $\ell_1(P)$ . Figure 14a, b presents the variation trends of vegetation  $P(t)$  of system (1.2) on  $t \in [0, 4000]$  (day), the frequency histogram of vegetation with the iteration time  $T_0 = 50,000$  days, and the function  $\ell_1(P)$  under the scenario RCP4.5. The corresponding simulations under the scenario RCP8.5 are shown in Fig. 14c, d. Analogous to Example 6.3, Fig. 15 shows the frequency histogram fitting curves of vegetation  $P$  at the iteration time equals to 10,000, 20,000 and 40,000 days of the total time  $T_0$ , each in a different color. By selecting 5000 equidistant observation points in the observation interval of the vegetation value in Fig. 15, Table 6 provides the corresponding values of some error types between the functions  $\ell_1(P)$  and  $\tilde{h}_1(P, \cdot)$ . In this example, it is clear to see that the local approximate marginal density  $\ell_1(P)$  has a good global fitting effect for the density function of the distribution  $\mu_1(P)$ . Furthermore, the vegetation state under the scenario RCP4.5 is more dense than that under the scenario RCP8.5, which implies that RCP4.5 may be a suitable climatic condition for vegetation growth than RCP8.5. Combining Figs. 3 and 4, one further obtains that as the global  $\text{CO}_2$  concentration rise, the climate conditions in Wuwei can be improved by implementing measures to increase annual precipitation, such as artificial rainfall, to improve the luxuriance and stability of vegetation in the future.



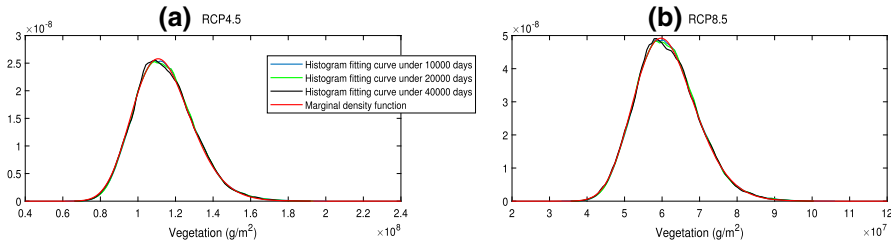


**Fig. 15** The blue, green and black lines separately denote the frequency histogram fitting curves of vegetation  $P$  with the iteration time equals to 10,000, 20,000 and 40,000 days of the total time  $T_0$ . The red lines represent the corresponding approximate density curve  $\ell_1(P)$  of vegetation  $P$ . All of the parameter values are the same as in Fig. 14

**Table 6** List of the errors  $e_a^{(m)}(P, \cdot)$ ,  $\bar{e}_a(P, \cdot)$  and  $\bar{e}_r(P, \cdot)$  of vegetation  $P$  at different iteration times (Fix parameters:  $\sigma_1 = 0.05$ ,  $\sigma_2 = \sigma_3 = 0.001$ )

Time interval $[0, T_0]$ (day)	$[0, 10,000]$	$[0, 20,000]$	$[0, 40,000]$
$e_a^{(m)}(P, \cdot)$ (RCP4.5)	$6.374 \times 10^{-10}$	$7.892 \times 10^{-10}$	$1.166 \times 10^{-9}$
$e_a^{(m)}(P, \cdot)$ (RCP8.5)	$1.581 \times 10^{-9}$	$1.423 \times 10^{-9}$	$2.537 \times 10^{-9}$
$\bar{e}_a(P, \cdot)$ (RCP4.5)	$2.478 \times 10^{-10}$	$3.054 \times 10^{-10}$	$6.142 \times 10^{-10}$
$\bar{e}_a(P, \cdot)$ (RCP8.5)	$4.251 \times 10^{-10}$	$5.626 \times 10^{-10}$	$7.865 \times 10^{-10}$
$\bar{e}_r(P, \cdot)$ (RCP4.5)	1.14%	1.36%	1.97%
$\bar{e}_r(P, \cdot)$ (RCP8.5)	1.32%	1.78%	2.57%

The observation interval:  $[0.4, 2.4] \times 10^8$  (RCP4.5) and  $[0.2, 1.2] \times 10^8$  (RCP8.5)

### 7 Discussions

In this paper, we investigate the interactions between the vegetation and two kinds of water environments including surface water and soil water. Taking the stochastic noise into account, a three-dimensional stochastic vegetation–water system (i.e., system (1.2)) is the first to be proposed and investigated, providing a mathematical feasible way for ecology research.

First, for its deterministic system (1.1), the local asymptotic stability of equilibria are obtained. Then for the stochastic system (1.2), we characterize the vegetation stability from both long-term and transient behavior perspectives. For the long-term behavior of vegetation, we obtain sufficient condition  $\mathcal{R}_0^H > 1$  for the existence and uniqueness of an ergodic stationary distribution  $\varpi(\cdot)$ . This implies that the vegetation will be persistent when  $\mathcal{R}_0^H > 1$ . Moreover, we define a quasi-endemic equilibrium  $\bar{D}^*$  of system (1.2). A novelty of this paper is that it theoretically derives an approximate expression (4.8) of the probability density function of the distribution  $\varpi(\cdot)$  around the equilibrium  $\bar{D}^*$ , and it has numerically shown that the local approximate density function  $\Upsilon(\cdot)$  in (4.8) has a good global fitting effect for the density function of the distribution  $\varpi(\cdot)$  under some small stochastic noises (see Figs. 7, 9, 15). For the transient behavior of vegetation, we establish sufficient condition  $\mathcal{R}_0^E < 1$  for the exponential extinction of vegetation. Another novelty of this paper is that it derives

the exact expression of the probability of vegetation extinction at any given time under  $\mathcal{R}_0^E < 1$ . Moreover, the maximum vegetation extinction time  $t_\epsilon^{(1-\delta)}$  in the sense of at least probability  $1 - \delta$  is obtained, and its rationality is verified based on some actual data from semi-arid ecosystems. Finally, both the theoretical results and numerical simulations show that the stochastic noises have a negative effect on vegetation density and stability, and may even lead to vegetation extinction. Thus, in practical terms, it is necessary to measure the environmental noise intensity to better monitor vegetation state and provide some effective strategies to maintain vegetation stability (via Theorems 3.1, 4.1, 5.1).

Several remaining interesting but challenging issues deserve further consideration. First, a value gap exists between the parameters  $\mathcal{R}_0^H$  and  $\mathcal{R}_0^E$ . In other words, for some sets of parameters satisfying neither Theorem 3.1 ( $\mathcal{R}_0^H > 1$ ) nor Theorem 5.1 ( $\mathcal{R}_0^E < 1$ ), the dynamical behavior of vegetation of system (1.2) is unknown. Thus, we need to explore other effective ways to close this value gap in the future. Second, the numerical simulations show a good global fitting effect of the local approximate density function  $\Upsilon(P, W, S)$  for some small stochastic noises. For better practical application, we need to investigate the continuous dependence on small stochastic noises of solution for Fokker–Planck equation, to obtain the global approximation error between  $\Upsilon(P, W, S)$  and the realistic density function of the distribution  $\varpi(\cdot)$  for the same initial distribution. This work is currently underway. Certainly, for some large stochastic noises, the corresponding approximate density function with good fitting effect should also be investigated and constructed. Furthermore, it is interesting to introduce other types of stochastic noise, such as impulsive perturbations (Zhang et al. 2020a; Wang et al. 2014), mean-reverting Ornstein–Uhlenbeck processes (Pan et al. 2022; Zhang and Yuan 2021; Zhao et al. 2015), colored noises (Zhang et al. 2020; Zhou et al. 2021), into system (1.2). The motivation is that the dynamics of vegetation may encounter sudden environmental changes and human interventions (Pan et al. 2020). To this end, based on the actual situation of different arid ecosystems, the corresponding vegetation–water system with suitable type of stochastic noise should be established and analyzed, and that is one of our future research directions.

**Acknowledgements** This work is supported by the National Natural Science Foundation of China (No. 11871473) and Shandong Provincial Natural Science Foundation (No. ZR2019MA010, ZR2019MA006).

**Data Availability** The data that support the findings of this study are available from the corresponding author upon reasonable request.

## Declarations

**Conflict of interest** The authors declare that they have no conflict of interest.

## Appendix A. (Local stability of system (1.1))

In this section, we will focus on the local stability of the equilibria  $D_0$  and  $D^*$  of system (1.1).

**Theorem A.1** *If  $\mathcal{R}_0 < 1$ , the vegetation-free equilibrium  $D_0$  of system (1.1) is locally asymptotically stable (LAS), but it is unstable when  $\mathcal{R}_0 > 1$ .*

**Proof** The Jacobi matrix of system (1.1) at the equilibrium  $D_0$  is

$$J(D_0) = \begin{pmatrix} R_{\text{esp}}(\mathcal{R}_0 - 1) & 0 & 0 \\ \frac{R(1-w_0)}{k_2 w_0} - \frac{q\gamma R_{\text{esp}} \mathcal{R}_0}{c} & -r_w & \alpha w_0 \\ -\frac{R(1-w_0)}{k_2 w_0} & 0 & -\alpha w_0 \end{pmatrix}.$$

By direct calculation, the characteristic polynomial of  $D_0$  is

$$\phi_{J(D_0)}(y) = [y - R_{\text{esp}}(\mathcal{R}_0 - 1)](y + r_w)(y + \alpha w_0).$$

Clearly,  $J(D_0)$  has three real eigenvalues  $y_1 = R_{\text{esp}}(\mathcal{R}_0 - 1)$ ,  $y_2 = -r_w < 0$  and  $y_3 = -\alpha w_0 < 0$ . If  $\mathcal{R}_0 < 1$ , then  $J(D_0) \in RH(3)$ . Combining Definition 2.1 and the Routh–Hurwitz criterion (Ma et al. 2015), we obtain that  $E_0$  is LAS when  $\mathcal{R}_0 < 1$ . Conversely, if  $\mathcal{R}_0 > 1$ , we get that  $y_1 = R_{\text{esp}}(\mathcal{R}_0 - 1) > 0$ , implying that  $D_0$  is unstable. This completes the proof of Theorem A.1.  $\square$

Next, we define a critical value by

$$\mathcal{R}_1 = \left[ \frac{c(R + r_w k_1)(\mathcal{R}_0 - 1)}{q\gamma(c\alpha_2 g_{\text{CO}_2} - R_{\text{esp}})} + k_2 w_0 \right]^2 - \frac{ck_2 R(1 - w_0)}{q\alpha\gamma}.$$

**Theorem A.2** *If  $\mathcal{R}_0 > 1$  and  $\mathcal{R}_1 \geq 0$ , the vegetation-positive equilibrium  $D^*$  is LAS.*

**Proof** Similar to Theorem A.1, the Jacobi matrix of system (1.1) at the equilibrium  $D^*$  is

$$J(D^*) = \begin{pmatrix} 0 & \frac{c\alpha_2 g_{\text{CO}_2} k_1 P^*}{(W^* + k_1)^2} & 0 \\ \frac{\alpha k_2 (1-w_0) S^*}{(P^* + k_2)^2} - \frac{q\alpha_2 \gamma g_{\text{CO}_2} W^*}{W^* + k_1} & -\frac{q\alpha_2 \gamma g_{\text{CO}_2} k_1 P^*}{(W^* + k_1)^2} - r_w & \frac{\alpha(P^* + k_2 w_0)}{P^* + k_2} \\ -\frac{\alpha k_2 (1-w_0) S^*}{(P^* + k_2)^2} & 0 & -\frac{\alpha(P^* + k_2 w_0)}{P^* + k_2} \end{pmatrix}$$

$$:= \begin{pmatrix} 0 & a_{12} & 0 \\ a_{21} & -a_{22} & a_{23} \\ a_{31} & 0 & -a_{23} \end{pmatrix},$$

where  $a_{12} = \frac{c\alpha_2 g_{\text{CO}_2} k_1 P^*}{(W^* + k_1)^2} > 0$ ,  $a_{21} = \frac{\alpha k_2 (1-w_0) S^*}{(P^* + k_2)^2} - \frac{q\alpha_2 \gamma g_{\text{CO}_2} W^*}{W^* + k_1}$ ,  $a_{22} = \frac{q\alpha_2 \gamma g_{\text{CO}_2} k_1 P^*}{(W^* + k_1)^2} + r_w > 0$ ,  $a_{23} = \frac{\alpha(P^* + k_2 w_0)}{P^* + k_2} > 0$  and  $a_{31} = \frac{\alpha k_2 (1-w_0) S^*}{(P^* + k_2)^2} > 0$ . A direct calculation shows that

$$\phi_{J(D^*)}(y) = y^3 + l_1 y^2 + l_2 y + l_3,$$

where  $l_1 = a_{22} + a_{23} > 0$ ,  $l_2 = a_{22} a_{23} - a_{12} a_{21}$  and  $l_3 = a_{12} a_{23} (a_{31} - a_{21})$ .

If  $\mathcal{R}_0 > 1$ , we determine that  $P^* = \frac{c(R+r_wk_1)(\mathcal{R}_0-1)}{q\gamma(c\alpha_2g_{CO_2}-R_{esp})}$  and  $a_{31} - a_{21} = \frac{q\alpha_2\gamma g_{CO_2}W^*}{W^*+k_1} > 0$ , which means that  $l_3 > 0$ . Moreover, if  $\mathcal{R}_1 \geq 0$ , by the equality  $R = \frac{\alpha(P^*+k_2w_0)S^*}{P^*+k_2}$ , we have

$$\begin{aligned} a_{22}a_{23} - a_{12}a_{31} &= \frac{\alpha(P^* + k_2w_0)}{P^* + k_2} \left[ \frac{q\alpha_2\gamma g_{CO_2}k_1P^*}{(W^* + k_1)^2} + r_w \right] \\ &\quad - \frac{c\alpha_2g_{CO_2}k_1k_2R(1 - w_0)P^*}{(W^* + k_1)^2(P^* + k_2)(P^* + k_2w_0)} \\ &\geq \frac{q\alpha\alpha_2\gamma g_{CO_2}k_1P^*}{(W^* + k_1)^2(P^* + k_2)(P^* + k_2w_0)} \\ &\quad \left[ (P^* + k_2w_0)^2 - \frac{ck_2R(1 - w_0)}{q\alpha\gamma} \right] \\ &= \frac{q\alpha\alpha_2\gamma g_{CO_2}k_1P^*\mathcal{R}_1}{(W^* + k_1)^2(P^* + k_2)(P^* + k_2w_0)} \geq 0. \end{aligned}$$

Combined with  $a_{21} < a_{31}$ , we obtain that  $l_2 = a_{22}a_{23} - a_{12}a_{21} > a_{22}a_{23} - a_{12}a_{31} \geq 0$  and

$$l_1l_2 - l_3 = a_{22}l_2 + a_{23}(a_{22}a_{23} - a_{12}a_{31}) \geq a_{22}l_2 > 0.$$

According to the Routh–Hurwitz criterion, we determine that  $J(D^*) \in \overline{RH}(3)$ . Thus,  $D^*$  is LAS when  $\mathcal{R}_0 > 1$  and  $\mathcal{R}_1 \geq 0$ . This completes the proof of Theorem A.2.  $\square$

### References

Beddington, J.R., May, R.M.: Harvesting natural populations in a randomly fluctuating environment. *Science* **197**(4302), 463–465 (1977)

Cai, Y., Kang, Y., Wang, W.: A stochastic SIRS epidemic model with nonlinear incidence rate. *Appl. Math. Comput.* **305**, 221–240 (2017)

Chen, Z., Wu, Y., Feng, G., Qian, Z., Sun, G.: Effects of global warming on pattern dynamics of vegetation: Wuwei in China as a case. *Appl. Math. Comput.* **390**, 125666 (2021)

Cox, P.M., Betts, R.A., Jones, C.D., et al.: Acceleration of global warming due to carbon-cycle feedbacks in a coupled climate model. *Nature* **408**, 184–187 (2000)

Dai, A.: Increasing drought under global warming in observations and models. *Nat. Clim. Change* **3**(1), 52–58 (2013)

Gao, M., Jiang, D., Hayat, T., Alsaedi, A.: Stationary distribution and extinction for a food chain chemostat model with random perturbation. *Math. Meth. Appl. Sci.* **44**, 1013–1028 (2021)

Gard, T.C.: *Introduction to Stochastic Differential Equations*. Marcel Dekker INC, New York (1988)

Gardiner, C.W.: *Handbook of Stochastic Methods for Physics, Chemistry and the Natural Sciences*. Springer, Berlin (1983)

Gilad, E., von Hardenberg, J., Provenzale, A., et al.: A mathematical model of plants as ecosystems engineers. *J. Theor. Biol.* **244**, 680–691 (2007)

Guttal, V., Jayaprakash, C.: Impact of noise on bistable ecological systems. *Ecol. Model.* **201**, 420–8 (2007)

Guttal, V., Jayaprakash, C.: Changing skewness: an early warning signal of regime shifts in ecosystems. *Ecol. Lett.* **11**, 450–60 (2008)

Han, Q., Yang, T., Zeng, C., et al.: Impact of time delays on stochastic resonance in an ecological system describing vegetation. *Phys. A* **408**, 96–105 (2014)

- Han, B., Jiang, D., Hayat, T., et al.: Stationary distribution and extinction of a stochastic staged progression AIDS model with staged treatment and second-order perturbation. *Chaos Soliton Fract.* **140**, 110238 (2020)
- Han, B., Jiang, D., Zhou, B., et al.: Stationary distribution and probability density function of a stochastic SIRS epidemic model with saturation incidence rate and logistic growth. *Chaos Soliton Fract.* **142**(5), 110519 (2020)
- Hautier, Y., Tilman, D., Isbell, F., et al.: Anthropogenic environmental changes affect ecosystem stability via biodiversity. *Science* **348**(6232), 336–340 (2015)
- Higham, D.J.: An algorithmic introduction to numerical simulation of stochastic differential equations. *SIAM Rev.* **43**, 525–546 (2001)
- Huang, J., Ji, M., Xie, Y., et al.: Global semi-arid climate change over last 60 years. *Clim. Dyn.* **46**, 1131–1150 (2016)
- Ikeda, N., Watanabe, S.: A comparison theorem for solutions of stochastic differential equations and its applications. *Osaka J. Math.* **14**, 619–633 (1977)
- Imhof, L., Walcher, S.: Exclusion and persistence in deterministic and stochastic chemostat models. *J. Differ. Equ.* **217**, 26–53 (2005)
- Jordan, R., Kinderlehrer, D., Otto, F.: The variational formulation of the Fokker–Planck equation. *SIAM J. Math. Anal.* **29**(1), 1–17 (1998)
- Kefi, S., Rietkerk, M., Katul, G.G.: Vegetation pattern shift as a result of rising atmospheric CO<sub>2</sub> in arid ecosystems. *Theor. Popu. Biol.* **74**, 332–344 (2008)
- Kefi, S., Eppinga, M.B., de Ruiter, P.C., Rietkerk, M.: Bistability and regular spatial patterns in arid ecosystems. *Theor. Ecol.* **3**, 257–269 (2010)
- Khasminskii, R.: *Stochastic Stability of Differential Equations*. Springer, Berlin (2011)
- Li, X., Liu, X., Ma, Z.: Analysis on the drought characteristics in the main arid regions in the world since recent hundred-odd years. *Arid Zone Res.* **21**, 97–103 (2004)
- Lin, Y., Jiang, D.: Threshold behavior in a stochastic SIS epidemic model with standard incidence. *J. Dyn. Differ. Equ.* **26**(4), 1079–1094 (2014)
- Lipster, R.: A strong law of large numbers for local martingales. *Stochastics* **3**, 217–228 (1980)
- Liu, Q., Jiang, D.: Periodic solution and stationary distribution of stochastic predator-prey models with higher-order perturbation. *J. Nonlinear Sci.* **28**, 423–442 (2018)
- Liu, Q., Jiang, D., Hayat, T., et al.: Dynamics of a stochastic predator-prey model with stage structure for predator and Holling Type II functional response. *J. Nonlinear Sci.* **28**, 1151–1187 (2018)
- Liu, C., Li, L., Wang, Z., Wang, R.: Pattern transitions in a vegetation system with cross-diffusion. *Appl. Math. Comput.* **342**, 255–262 (2019)
- Liu, Q., Jiang, D., Hayat, T., et al.: Stationary distribution and extinction of a stochastic HIV-1 infection model with distributed delay and logistic growth. *J. Nonlinear. Sci.* **30**(1), 369–395 (2020)
- Liu, G., Qi, H., Chang, Z., Meng, X.: Asymptotic stability of a stochastic May mutualism system. *Comput. Math. Appl.* **79**(3), 735–745 (2020)
- London, N., Unep, N.: United nations convention to combat desertification in countries experiencing serious drought and/or desertification, particularly in Africa. Document A/AC. 241/27, 12.09.1994 with Annexes. New York, NY (1994)
- Ma, Z., Zhou, Y., Li, C.: *Qualitative and Stability Methods for Ordinary Differential Equations*. Science Press, Beijing (2015). (in Chinese)
- Mao, X.: *Stochastic Differential Equations and Applications*. Horwood Publishing, Chichester (1997)
- Marinov, K., Wang, T., Yang, Y.: On a vegetation pattern formation model governed by a nonlinear parabolic system. *Nonlinear Anal. Real World Appl.* **14**, 507–525 (2013)
- May, R.M.: Thresholds and breakpoints in ecosystems with a multiplicity of stable states. *Nature* **269**(5628), 471–477 (1977)
- Nguyen, D.H., Yin, G., Zhu, C.: Long-term analysis of a stochastic SIRS model with general incidence rates. *SIAM J. Appl. Math.* **80**, 814–838 (2020)
- Pan, S., Zhang, Q., Anke, M.: Near-optimal control of a stochastic vegetation–water system with reaction diffusion. *Math. Meth. Appl. Sci.* **43**(9), 6043–6061 (2020)
- Pan, S., Zhang, Q., Anke, M.: Stationary distribution of a stochastic vegetation–water system with reaction–diffusion. *Appl. Math. Lett.* **123**, 107589 (2022)
- Roosen, H.: An asymptotic solution to a two-dimensional exit problem arising in population dynamics. *SIAM J. Appl. Math.* **49**, 1793 (1989)

- Saco, P.M., Willgoose, G.R., Hancock, G.R.: Eco-geomorphology of banded vegetation patterns in arid and semi-arid regions. *Hydrol. Earth Syst. Sci.* **11**, 1717–1730 (2007)
- Shnerb, N.M., Sarah, P., Lavee, H., Solomon, S.: Reactive glass and vegetation patterns. *Phys. Rev. Lett.* **90**(3), 038101 (2003)
- Sun, G., Li, L., Zhang, Z.: Spatial dynamics of a vegetation model in an arid flat environment. *Nonlinear Dyn.* **73**(4), 2207–2219 (2013)
- Wang, F., Wang, X., Zhang, S., Ding, C.: On pulse vaccine strategy in a periodic stochastic SIR epidemic model. *Chaos Soliton Fract.* **66**, 127–135 (2014)
- Yang, D., Liu, Y., Cai, Z., et al.: The spatial and temporal distribution of carbon dioxide over China based on GOSAT observations. *Chin. J. Atmos. Sci.* **40**(3), 541–550 (2016)
- Zhang, X., Yuan, R.: A stochastic chemostat model with mean-reverting Ornstein–Uhlenbeck process and Monod–Haldane response function. *Appl. Math. Comput.* **394**, 125833 (2021)
- Zhang, H., Zhang, T.: The stationary distribution of a microorganism flocculation model with stochastic perturbation. *Appl. Math. Lett.* **103**, 106217 (2020)
- Zhang, H., Xu, W., Lei, Y., Qiao, Y.: Early warning and basin stability in a stochastic vegetation–water dynamical system. *Commun. Nonlinear. Sci. Numer. Simul.* **77**, 258–270 (2019)
- Zhang, H., Liu, X., Xu, W.: Threshold dynamics and pulse control of a stochastic ecosystem with switching parameters. *J. Frankl. Inst.* **358**(1), 516–532 (2020)
- Zhang, H., Xu, W., Han, P., Qiao, Y.: Stochastic dynamic balance of a bi-stable vegetation model with pulse control. *Phys. A* **556**, 124809 (2020)
- Zhang, H., Xu, W., Guo, Q., et al.: First escape probability and mean first exit time for a time-delayed ecosystem driven by non-Gaussian colored noise. *Chaos Soliton Fract.* **135**, 109767 (2020)
- Zhao, Y., Yuan, S., Ma, J.: Survival and stationary distribution analysis of a stochastic competitive model of three species in a polluted environment. *Bull. Math. Biol.* **77**(7), 1285–1326 (2015)
- Zhou, B., Jiang, D., Dai, Y., et al.: Stationary distribution and probability density function of a stochastic SVIS epidemic model with standard incidence and vaccination. *Chaos Soliton Fract.* **143**, 110601 (2021)
- Zhou, B., Han, B., Jiang, D., et al.: Ergodic stationary distribution and extinction of a hybrid stochastic SEQIHR epidemic model with media coverage, quarantine strategies and pre-existing immunity under discrete Markov switching. *Appl. Math. Comput.* **410**, 126388 (2021)
- Zhu, C., Yin, G.: Asymptotic properties of hybrid diffusion systems. *SIAM J. Control. Optim.* **46**, 1155–1179 (2007)
- Zu, L., Jiang, D., O’Regan, D., et al.: Ergodic property of a Lotka–Volterra predator–prey model with white noise higher order perturbation under regime switching. *Appl. Math. Comput.* **330**, 93–102 (2018)

**Publisher’s Note** Springer Nature remains neutral with regard to jurisdictional claims in published maps and institutional affiliations.